Università degli Studi di Salerno

Dipartimento di Ingegneria Elettronica ed Ingegneria Informatica

Dottorato di Ricerca in Ingegneria dell'Informazione
X Ciclo – Nuova Serie

TESI DI DOTTORATO

Electromagnetic Characterization and Modeling of CNT-based Composites for Industrial Applications

CANDIDATO: **GIOVANNI SPINELLI**

TUTOR: **ING. PATRIZIA LAMBERTI**
CO-TUTOR: **PROF. LUIGI EGIZIANO**

COORDINATORE: **PROF. ANGELO MARCELLI**

Anno Accademico 2010 – 2011

There's Plenty of Room at the Bottom

Richard Feynman, 1959.

Contents

List of Figures

List of Tables

X

Introduction

In several applications for the aeronautic, automotive and electronic industries, there is an increasing demand of structural nanocomposites exhibiting remarkable thermal and mechanical properties and, at the same time, tailored and controlled electromagnetic (EM) performances.

Along this stream, an intense research activity has been carried out focused at producing new polymeric nanocomposites based on Carbon NanoStructures (CNSs) such as Carbon NanoTubes (CNTs) and NanoFibres (CNFs). This thesis concerns the electromagnetic characterization and modeling of nanostructured polymeric materials based on CNT and CNT/nanoclays.

The interest and the scientific importance of the topic is justified by the fact that the conventional materials do not have the suitable properties to satisfy the specific requirements for modern applications.

Instead, two or more distinct materials may be combined to form a material which possesses superior properties, with respect to those of individual components.

Thus the individuation and preparation of advanced composites with best features respect to the traditional materials is currently required in several industrial sectors [1].

In this context, a particular class of composite systems of materials known as nanocomposites or nanostructured materials, in which a component has at least one dimension of the order of nm, are currently object of a fervent interest in science and technology.

Since their first observation [2], research efforts have been widely oriented on the study of Carbon NanoTubes (CNTs) for their unique properties in terms of electron mean-free path, current carrying capability and thermal and mechanical stability.

For these remarkable benefits they were identified as the most important and promising nanomaterials and in recent years, the interest in nanostructures with carbon nanotubes has grown considerably.

Typically, important applications are for example as antistatic elements, electrostatic dissipative ones or for electromagnetic shielding in the field of the aeronautic, automotive and electronic

industries where electrically conductive polymeric materials, originally insulation, play an important role.

One of the most significant aspects that can be found as a consequence of the introduction of a conductive nanofiller is the variation of the electrical conductivity of polymeric material as function of volume fraction of the filler (filler loading).

Gradually, with increasing fraction of additives, as soon as it reaches a certain concentration (known as percolation threshold), electrical conductivity undergoes a significant increase of several orders of magnitude and then varies only slightly with further increases of filler [3].

Since CNTs can be exploited with varying structural and physical properties, geometry and functionality, the possible range of composite material properties can be very large [4]. In order to analyse such properties and design components based on nanocomposites with improved performances the experimental electromagnetic characterization of the composites has to be complemented with suitable models able to correlate structural and electrical characteristics. In fact, a complete understanding of the relations linking the electrical properties with the geometrical and physical characteristics of the composite and the topological structures formed is still to be achieved. Therefore, additional efforts aimed at providing further information on the dependencies among electrical characteristics and the above mentioned parameters seems valuable.

In this framework, the research project carried out during the PhD program has been focused on two main aspects: the electromagnetic characterization of nanocomposite materials (epoxy-CNT and epoxy-CNT-clay) and the development of an accurate numerical model which can be used to obtain information on the composite properties once some geometrical and physical properties (both of CNT and matrix) are identified.

A correlation between the results of the extensive experimental investigations with predictions obtained by a suitable numerical model has been performed. A versatile and realistic 3D model of the structures obtained by randomly mixing conducting cylinders inside an insulating cubic matrix has been developed. The variation of the electrical conductivity of the structure for different volume loadings of the conducting phase can be estimated by implementing a 3D resistor

network which includes resistors associated to the tunneling effect between conducting clusters. By using a Monte Carlo analysis the behavior of the electrical conductivity and the dependence of the percolation thresholds as a function of geometrical and physical influencing parameters can be carried out. In particular, the filler concentration, the filler aspect ratio (i.e. the ratio between length and diameter) and the height of the energy barrier of tunneling conduction have been considered.

The results of numerical simulations are in good agreement with those obtained from the experimental characterization. This thesis is organized as follows:

- in the first chapter an overview on the state of art on the production techniques, properties, and the most promising applications of CNT is briefly reported.
- some fundamental phenomena underlying the performances of nanocomposites, such as percolation, responsible for the change in conductivity and "tunneling" conduction in these materials are discussed in the second chapter [5].
- in the third chapter, the results concerning the extensive experimental characterization both in the time and frequency domain on nanocomposites containing different concentrations of CNT and CNT-clay, is described in detail relative to samples. The possible influence of the morphological characteristics on the electrical behavior of the composite is studied.
- The last chapter provides an overview on the models available in the literature and then presents the numerical model that has been implemented. A detailed description of the model, both in terms of geometric approach and the optimization algorithm is given. The simulation results obtained by such a model are provided and compared with literature data and with experimental results obtained from the characterization described in the previous chapter. The ability to provide

information on the electromagnetic behavior of CNT based composites is checked.

- Finally, conclusions and future work are presented.

References

[1] A. Lagashetty, A. Venkataraman “Polimer Nanocomposites”, Resonance, Volume 10, Number 7, 49-57, July 2005
[2] Iijima, S., ‘‘Helical Microtubles of Graphitic Carbon,’’ Nature (London), 354, pp. 56–58, 1991,
[3] C.W.Nan, Y. Shen,2 and Jing Ma, “Physical Properties of Composites Near Percolation”, Annu. Rev. Mater. Res. 40, pp131–151, 2010.
[4] L.Guadagno et al., Cure behavior and physical properties of epoxy resin-filled with multiwalled carbon nanotubes, Journal of Nanoscience and Nanotechnology 10(4) (2010) 2686-2693.
[5] C. Ly et al., Dominant role of tunnelling resistance in the electrical conductivity of carbon nanotube-based composites, Applied Physics Letters 91, 2007

Chapter 1

Carbon nanotubes: structure and properties

This chapter is devoted to the description of carbon nanotube (CNT) unique properties that make them suitable materials for different applications and particularly excellent constituents of composite materials. The main forms and characteristics of CNT, namely Multi Wall and Single Wall CNTs are presented. The properties, and in particular the electrical conductivity of CNTs, are derived.

1.1 Carbon nanotube

Carbon nanotubes were discovered accidentally in 1991 by Japanese physicist Sumio Iijima [1] in the laboratories of the NEC[1]. By using an High Resolution Transmission Electron Microscopy, (HR-TEM[2]) he observed as on the negative electrode of the apparatus used for the production of fullerenes are also deposited nano-tubular structures of graphite. These structures were called nanotubes (see Fig.1.1) For a complete understanding of their geometrical and

[1] **NEC:**, a Japanese multinational IT company, has its headquarters in Minato, Tokyo, Japan.NEC, part of the Sumitomo Group, provides information technology (IT) and network solutions to business enterprises, communications services providers and government. The company used the name Nippon Electric Company, Limited before re-branding in 1983.

[2] **HR-TEM:** is an imaging mode of the transmission electron microscope (TEM) that allows the imaging of the crystallographic structure of a sample at an atomic scale using an electron beam transmitted through a sample ultra-thin. The image, formed by electrons transmitted, is magnified and focused on one objective lens. At present, the highest resolution realised is 0.8 Å. At these small scales, individual atoms and crystalline defects can be imaged.

physical characteristics as well as the electronic properties, it is essential the introduction of the carbon as chemical element or , the graphite , one of its allotropic forms.

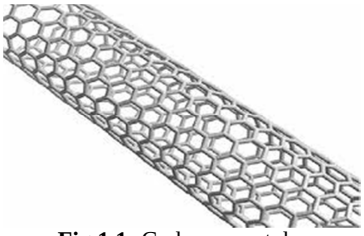

Fig.1.1: Carbon nanotube

1.1.1 Carbon: the chemical element

Carbon (chemical symbol C) is the sixth element of the periodic table (fourth group, the second period) [2].

It is a non-metal and has four electrons in its outer shell with an electronic configuration $1s^2 2s^2 2p^2$. Carbon is present in nature both in the free state that in the form of compounds, among which calcite ($CaC0_3$) and dolomite ($CaMg(CO_3)_2$), and it represents the 0.2% of the terrestrial crust. Carbon is also present in the air as carbon dioxide (CO_2) in the percentage of 0.04% and it is also the key component of the tissues of all known life forms.

It is the 15^{th} most abundant element on the earth and the fourth most abundant element in the universe by mass after hydrogen, helium, and oxygen.

The atom of carbon can reach a stable configuration forming four covalent bonds.

Each atom can form single, double or triple bonds, using various hybridization orbitals and it is unique among the elements for the extent with which form bonds between identical atoms and for the great variety of compounds in which it participates. The carbon atoms form long chains, branched chains and rings, which in turn may also have chains.

In an isolated atom, the electrons are arranged in their orbits so that the atom has the lowest energy.

Therefore, two electrons in the carbon occupy the inner orbital *1s* and do not participate in chemical bonds, while the remaining four (valence electrons) occupy the outer orbitals 2*s*, 2*p* (valence shell) and are responsible for chemical bonds that are formed.

When there are other nearby carbon atoms, each carbon atom can combine its valence orbitals to form a new group of orbitals that, in the presence of other atoms has a lower total energy than it would have its pure atomic orbitals .

This process is called hybridization and the new orbitals formed are called hybrid orbitals. These hybrid orbitals can overlap with other hybrid orbitals of carbon atoms in order to share electrons and to form covalent bonds.

In an atom of carbon, the *2s* orbital can hybridize with one, two or all three the *2p* orbitals forming, respectively, two *sp* hybrid orbitals, three sp^2 hybrid orbitals, four sp^3 hybrid orbitals which have higher energy orbital than the *2s* but less than the *2p* orbitals of origin.

At the elemental state, the carbon can be in the amorphous form or have crystalline structure. In the latter case with different molecular configurations called “allotropes”. The three relatively well-known allotropes of carbon (see Fig.1.2) are diamond, graphite, and fullerenes which, although having the same basic chemical elements, have different characteristics due to the several interactions between adjacent carbon atoms.

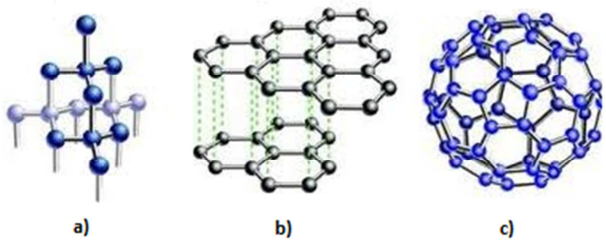

Fig.1.2: Some allotropes of carbon: a) diamond; b) graphite; c) fullerenes

The allotropes of carbon varies substantially in the orbital hybridization of the atoms involved, so that the graphite and fullerene

have sp^2 hybridization while diamond has sp^3 hybridization. Below we see the characteristics of the allotropic forms.

1.1.2 Graphite-graphene

From a structural viewpoint (Fig.1.3), the carbon atoms form a hexagonal lattice in layers, with σ bonds and π bonds[3] within each layer, while other layers are held together with each other through Van der Waals forces[4] [3].

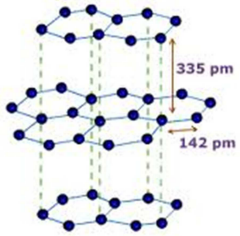

Fig.1.3: Crystal structure of graphite

When the atoms are sp^2 hybridized and the bonds are arranged on the same plane separated by 120 ° is obtained a planar hexagonal lattice called " graphene" (Fig.1.4).

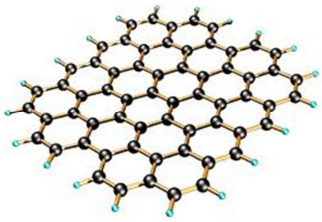

Fig.1.4: Structure of graphene

[3] **π bonds:** in chemistry, are covalent chemical bonds where two lobes of one involved electron orbital overlap two lobes of the other involved electron orbital. Only one of the orbital's nodal planes passes through both of the involved nuclei**.** Pi bonds are usually weaker than sigma bonds and electrons in pi bonds are sometimes referred to as pi electrons.

[4] **Van der Waals forces:** or London dispersion forces are weak intermolecular attractions a short-range between molecules non-polar due to the continuous movement of electrons in the molecules that lead to a symmetrical distribution of electrical charges by allowing the formation of instantaneous dipoles.

Therefore, the graphite can be considered as the overlapping of parallel graphene sheets placed at a distance of 3.4 Å.

The sigma bonds of the sp^2 orbital is long 1.5 Å and strong 360 kcal/mol, which makes graphite harder than diamond in the plan. However, due of the weak interactions of van der Waals forces, graphene sheets tend to slide the each other making the graphite soft, crumbly and reducible to dust.

Graphite can conduct electricity due to the vast electron delocalization within the carbon layers (a phenomenon called aromaticity[5]) [4]. The π-electrons are free to move, so are able to conduct electricity and their interactions with light make up the graphite of a black color.

The findings on graphene and its applications (production of a transistor) achieved in 2004 , have given in 2010 the Nobel Prize for physics to two physicists Andre Geim and Novoselov Konstantin of the University of Manchester.

Despite the initial problems encountered in the applicability of the single-layer graphene, the two physicists have developed the material to the construction of so-called bilayer graphene, which provides extra strength and applicability of use.

1.2 Carbon nanotubes structure

The easiest way to understand the structure is to think of sheets of graphene rolled up on themselves to form a series of coaxial cylinders (Fig.1.5) in which, eventually, the ends may be closed by two semi-spherical fullerene caps (end caps, Fig.1.6).

[5] **Aromaticity:** in organic chemistry, the structures of some rings of atoms are unexpectedly stable. Aromaticity is a chemical property in which a conjugated ring of unsaturated bonds, lone pairs, or empty orbitals exhibit a stabilization stronger than would be expected by the stabilization of conjugation alone. It can also be considered a manifestation of cyclic delocalization and of resonance

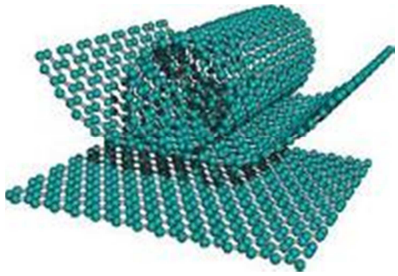

Fig.1. 5: Generation of the nanotube from sheets of graphene

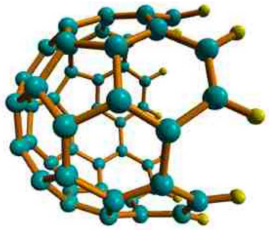

Fig.1.6: End caps of a CNT. It is possible to note how the pentagonal cells contribute to the decrease the diameter of nanotube (forcing the wall to the inside) until the close.

The creation of such structures is explained as a consequence of the high reactivity of the many "free" bonds (dangling-bond[6]) that characterize the edges of graphene layers of finite size [5]. The formation of curved tubular structures generally leads to the stabilization of the system but also, however, a relative increase of the stress-energy tensor[7].

The nanotubes observed initially by Iijima were multi-walled type, whose meaning will be clarified soon, and are shown in Fig.1.7.

---

[6] **Dangling-bond:** in chemistry, is an unsatisfied valence on an immobilised atom. In order to gain enough electrons to fill their valence shells (see also octet rule), many atoms will form covalent bonds with other atoms. In the simplest case, that of a single bond, two atoms each contribute one unpaired electron, and the resulting pair of electrons is shared between both atoms

[7] **Stress-energy tensor:** in the non-planar conjugated organic molecules derived from two main sources:
- by the pyramidalization of conjugated carbon atoms
- from the imperfect alignment of the π-orbitals of the atoms of carbon adjacent

The non-alignment of the π-orbitals in the nanotubes is the primary source of the stress-energy tensor

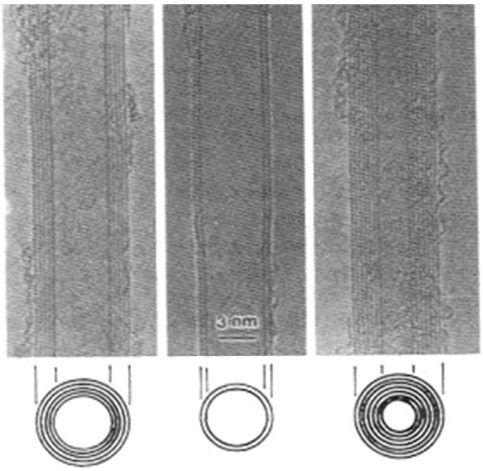

Fig.1.7: TEM images of multi-walled nanotubes observed by Iijima.

As in the graphite, in each carbon atom forming the nanotube there are three orbital sp^2 hybrid slightly deformed that determine the three covalent bonds with adjacent atoms. The circular curvature of the nanotubes causes a qu3antum confinement and a re-hybridization σ-π of the orbitals: the resulting σ-bonds are not longer completely planar and the π-electrons are more delocalized to the outside of the tube.

This makes nanotubes mechanically stronger, more conductive both electrically and thermally and chemically most active of the graphite.

An ideal nanotube is composed of walls formed by a hexagonal lattice. In reality, however, nanotubes have often structural defects and imperfections in the geometric structure.

So, in a nanotube defective there are topological defects such as pentagons and octagons, or other chemical and structural diversity.

However, these structural defects allow to obtain closed, helical or toroidal nanotubes (Fig.1.8), and to modify the electrical, optical and mechanical behavior of the nanotubes allowing the realization of nanoscale metal-semiconductor junctions, metal-insulator, etc.

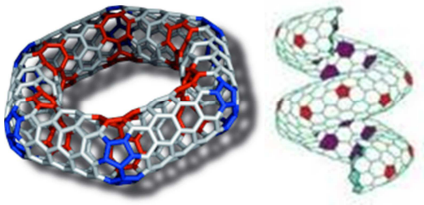

Fig.1. 8: Other geometries of the nanotubes(toroidal left, helical right)

Carbon nanotubes can be of two different types:

- Single Walled Carbon Nanotube (SWCNT) that consists of a single sheet of graphene rolled up (Fig.1.9 a);
- Multi Walled Carbon Nanotube, (MWCNT) are originated from more SWCNT with an increasing radius and arranged coaxially (Fig. 1.9 b) at a distance of 0.34 nm (distance of van der Walls[8]). In MWCNT are present some contacts between the various walls (lip-lip interactions) that seem to stabilize the growth of these nanotubes [6].
-

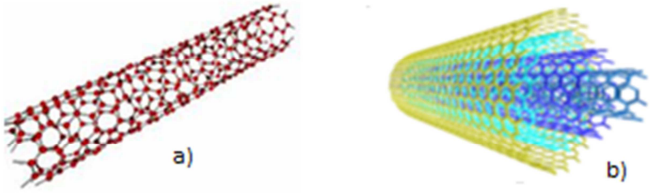

Fig.1. 9: Structures of carbon nanotubes: a) SWCNT; b) MWCNT

Nanotubes are often collected in bundles (for both types) as depicted in Fig.1.10, [7].

[8] **Distance of van der Walls:** also radius of van der Walls, rw, of an atom is the radius of an imaginary hard sphere which can be used to model the atom for many purposes. It is named after Johannes Diderik van der Waals, winner of the 1910 Nobel Prize in Physics, as he was the first to recognise that atoms had a finite size (i.e., that atoms were not simply points) and to demonstrate the physical consequences of their size through the van der Waals equation of state.

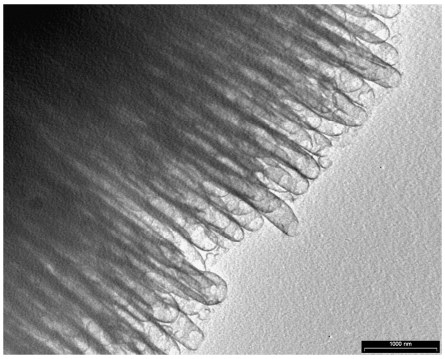

Fig.1. 10: SEM images of bundles of carbon nanotubes [7].

1.2.1 SWCNT

The first SWCNTs were produced in 1993, two years later the MWCNTs, by means of an electric arc system with electrodes composed of a mixture carbon-cobalt [8].

While the body of the nanotube consists of only hexagons, the end caps consist of hexagons and pentagons, like normal fullerenes, so as to bind perfectly to the cylindrical structure of the tube.

For this reason, the SWCNT can be considered as a sort of "giant fullerenes", and are therefore also called "buckytubes"

Regarding the geometry, the diameter of a SWCNT in most cases varies between 0.6 nm and 2 nm, but also SWCNT were observed with a minimum diameter of 0.4 nm and a maximum of 3 nm.

The SWCNT have an aspect ratio varying between 10^3 and 10^5 [9].Now, when a sheet of graphite rolled up, can do it with different possible directions. Considering the constraint of cylindrical symmetry, we can close the paper only in a discrete number of directions to form the nanotube. For a better understanding of the geometric characterization of CNT consider a graphene sheet lying on a plane as in Figure 1.11.

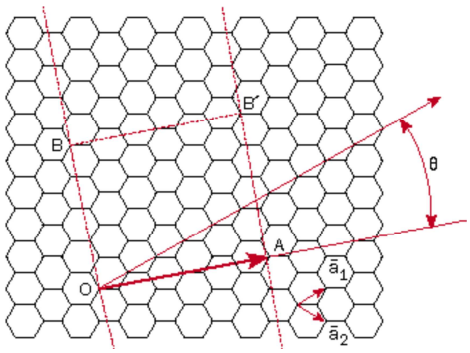

Fig.1.11: Structure of a graphene sheet with highlighted: the chiral vector OA, the chiral angle θ, the direction of the nanotube axis OB, the unit cell OAB'B and the unit vectors a_1 and a_2

Diameter and chiral vector (or helicity) $\bar{c}$, defined as the direction of rolling of the graphite respect to the tube axis, are needed to characterize a SWCNT.

The chiral vector connects two equivalent crystallographic sites and it is specified respect to primitive vectors a_1, a_2 of the lattice of graphene:

$$C = na_1 + ma_2 \qquad 1.1$$

where the pair of integers (n, m) are called chiral indices and used to identify the type of SWCNT as will be clarified soon.

Considered a Cartesian reference system (x,y), the analytical equations of the primitive vectors are:

$$a_1 = \left(\frac{\sqrt{3}}{2}a, \frac{a}{2}\right), a_2 = \left(\frac{\sqrt{3}}{2}a, -\frac{a}{2}\right) \qquad 1.2$$

where a = $|a_1|=|a_2|$=246nm is the lattice constant of graphene and it is linked to a_0 = 0:142 nm, length of the bond between two adjacent carbon atoms, through the relation:$a = \sqrt{3}a_0$ [10].

The chirality influences the conductance of the nanotube, its lattice structure and other properties. Moreover, given the chiral vector, it is possible to determine the diameter of the nanotube, by using the relation:

$$d = \frac{|C|}{\pi} = \frac{\sqrt{3}}{\pi}a_0\sqrt{n^2 + nm + m^2} \qquad 1.3$$

The angle θ formed between the vector chiral *C* and the vector a_1 is called chiral angle. It is expressed by the following relation:

$$\vartheta = tan^{-1}\left(\frac{\sqrt{3}m}{m+2n}\right) \qquad 1.4$$

The vector *T* normal to *C* and parallel to the axis of the nanotube is called *translation vector* and describes the distance between two equivalent points of the lattice. Its analytical expression is as follows:

$$T = t_1 a_1 + t_2 a_2 \qquad 1.5$$

where t_1 and t_2 are integer.

The vectors *C* and *T* define the two-dimensional cell of the nanotube. The cylinder is obtained by overlapping two ends of the vector *C*.

The electrical properties of nanotubes depend strongly to the chirality of the nanotube, i.e., the indices *n* and *m*. In particular, as depicted in Fig.1.12, we can distinguish:

- *zig-zag* nanotube, with *n* or *m* = 0 and $\theta = 0°$;
- *armchair* nanotube, with *n* =*m* and $\theta = 0°$;
- *chiral* nanotube, with [$n \neq$ m] ≠0 and $0° < \theta < 30°$;

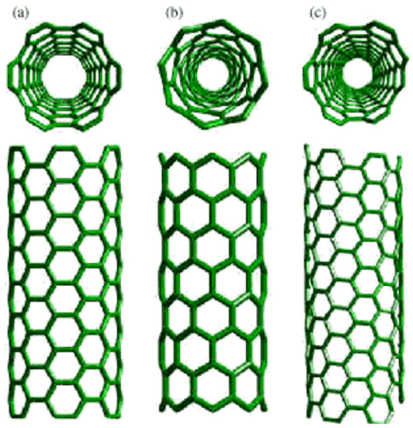

Fig.1. 12: Types of nanotubes: a) armchair; b) ziz-zag; c) chiral

1.2.2 MWCNT

The MWCNTs are composed by several SWCNTs, in this case indicated as shell or wall of the MWCNTs, arranged with different diameters and chirality in coaxial way at a minimum distance which is that imposed by Van der Walls' interaction.

There are two distinct theories that explain the formation of MWCNT:

- *Russian Doll Model*, for which the MWCNT is made up of graphene wrapped to form concentric cylinders like dolls;
- *Parchment Model*, for which a single layer of graphene is wrapped around itself several times as a sheet of parchment.

Anyway, the minimum diameter observed is about 0.4 nm and it can typically vary up to a maximum of 100nm because when the size of MWCNT become relatively large, it is considered as a special case of a tubular fiber.

The Double Walled Carbon Nanotubes (DWCNTs) represent a special case of MWCNTs in which the number of shells is just reduced to two. However, their properties are similar to those of SWCNTs but the presence of an additional wall increases their resistance to attack by chemical agents, making them more indicated in cases that require functionalization[9] of the nanotube, which allows give new and interesting properties to the same [11].

Essentially, the MWCNTs have the following advantages:

- growth in the absence of catalytic particles and this is a benefit because transition metals as Fe, Co, Ni have well known toxicity to humans;
- greater resistance to chemical agents used to functionalize the nanotube;
- greater strength exhibited by the structure, useful for use as tips for STM[10] / AFM[11][12].

---

[9] **Functionalization:** This treatment, which consists in the chemicals graft on the surface of the nanotube, leads to the break of a number of C-C bonds, and the structural defects resulting can change the physical properties of the nanotube. In the case of SWCNTs only the outer shall undergoes this process and the changes are less drastic.

[10] **STM:** A scanning tunneling microscope (STM) is an instrument for imaging surfaces at the atomic level. Its development in 1981 earned its inventors, Gerd Binnig and Heinrich Rohrer (at IBM Zürich), the Nobel Prize in Physics in 1986.For an STM, good resolution is considered to be 0.1 nm lateral

The outer diameter of the MWCNTs depends on the growth process.

1.3 Carbon nanotube: electronic properties

To study the electronic properties of carbon nanotubes must be first analyze the properties of a single sheet of graphene, from which it is possible to understand the behavior of such structures [13],[14],[15].

1.3.1 Band structure of graphene

The electronic properties of graphene depend on its particular band structure. The band structure of a two-dimensional lattice is described in terms of the wavevector k = (k_x, ky) and the area that includes all values of k associated with a given energy band is a Brillouin zone[12].

---

resolution and 0.01 nm depth resolution.[3] With this resolution, individual atoms within materials are routinely imaged and manipulated. The STM can be used not only in ultra high vacuum but also in air, water, and various other liquid or gas ambients, and at temperatures ranging from near zero kelvin to a few hundred degrees Celsius.
The STM is based on the concept of quantum tunnelling. When a conducting tip is brought very near to the surface to be examined, a bias (voltage difference) applied between the two can allow electrons to tunnel through the vacuum between them. The resulting tunneling current is a function of tip position, applied voltage, and the local density of states (LDOS) of the sample.[4] Information is acquired by monitoring the current as the tip's position scans across the surface, and is usually displayed in image form. STM can be a challenging technique, as it requires extremely clean and stable surfaces, sharp tips, excellent vibration control, and sophisticated electronics.

[11] **AFM:** Atomic force microscopy (AFM) or scanning force microscopy (SFM) is a very high-resolution type of scanning probe microscopy, with demonstrated resolution on the order of fractions of a nanometer, more than 1000 times better than the optical diffraction limit. Binnig, Quate and Gerber invented the first atomic force microscope (also abbreviated as AFM) in 1986. The first commercially available atomic force microscope was introduced in 1989. The AFM is one of the foremost tools for imaging, measuring, and manipulating matter at the nanoscale. The information is gathered by "feeling" the surface with a mechanical probe. Piezoelectric elements that facilitate tiny but accurate and precise movements on (electronic) command enable the very precise scanning. In some variations, electric potentials can also be scanned using conducting cantilevers. In newer more advanced versions, currents can even be passed through the tip to probe the electrical conductivity or transport of the underlying surface, but this is much more challenging with very few research groups reporting reliable data.

[12] **Brillouin zone:** In mathematics and solid state physics, it is a uniquely defined primitive cell in reciprocal space. The boundaries of this cell are given by planes related to points on the reciprocal lattice.

As shown in Fig.1.13 (a), the structure of graphene consists of carbon atoms arranged in a hexagonal lattice and the primitive cell, described by the vectors a_1 and a_2, contains two carbon atoms. In the same figure the dashed hexagon is the unit cell of graphene and the points 1 and 2 represent two carbon atoms.

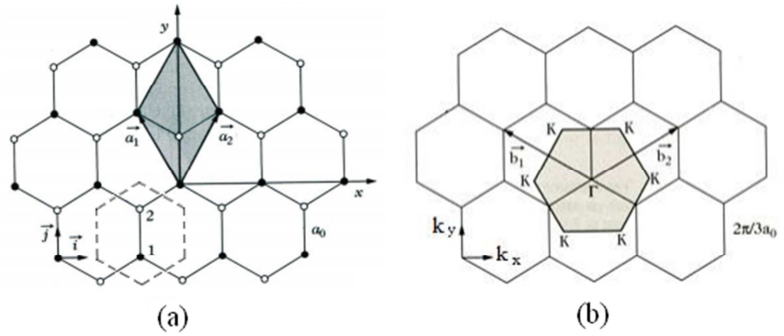

Fig.1.13: (a) Direct lattice of graphene. (b) Reciprocal lattice of graphene

The conversion from this lattice, described by vectors a_i in the spatial plane (x, y), to the reciprocal one described by vectors b_j in the plane of the wavevector (k_x, k_y) is allowed if the following conditions are met:

$$a_i \cdot b_j = 2\pi\delta_{ij} = \begin{cases} 2\pi, & if\ i = j \\ 0, & if\ i \neq j \end{cases} \qquad 1.6$$

Rewriting the expression of a_1, a_2 as a function of a_0 in the reference system shown in Fig.1.20 the following relations can be obtained:

$$a_1 = \left(-\frac{\sqrt{3}a_0}{2}, \frac{3}{2}a_0\right), a_2 = \left(\frac{\sqrt{3}a_0}{2}, \frac{3}{2}a_0\right) \qquad 1.7$$

$$b_1 = \left(-\frac{2\pi}{\sqrt{3}a_0}, \frac{2\pi}{3a_0}\right), b_2 = \left(\frac{2\pi}{\sqrt{3}a_0}, \frac{2\pi}{3a_0}\right) \qquad 1.8$$

The importance of the Brillouin zone stems from the Bloch wave description of waves in a periodic medium, in which it is found that the solutions can be completely characterized by their behavior in a single Brillouin zone.

The band structure of graphene can be evaluated using the approximation of Tight Binding Approximation (or TB model). This approach allows to explain the conduction properties of most of the regular solids. A orbital function of the crystal, which describes the electron in the periodic field of the entire crystal, is built starting from the wave function for an electron in a free atom. The wave function of the solid is determined by a linear combination of atomic wave functions (Linear Combination of Atomic Orbitals).

In determining the band structure of graphene are considered only the electrons π since they are the only ones to determine the transport properties of graphene. In fact, these electrons are weakly bound and therefore a small energy is enough to free them and bring them in conduction. Since there are two such electrons per unit cell, they produce two bands of type π identified as type π and π*.

The dispersion relation E (k) obtained for the graphene sheet is:

$$E(k) = \pm\beta\sqrt{3 + 2\cos[k(a_1 - a_2)] + 2\cos(k \cdot a_1) + 2\cos(k \cdot a_2)} \quad 1.9$$

where β is the interaction term of neighboring points.

Moreover, the dispersion relation can be expressed as a function of the components k_x, k_y,of the wavevector *k.*

$$E(k_x, k_y) = \pm\beta\sqrt{1 + 4cos\left(\frac{a\sqrt{3}}{2}k_y\right)cos\left(\frac{a}{2}k_y\right) + 4cos^2\left(\frac{a}{2}k_x\right)} \quad 1.10$$

with $a = |a_1| = |a_2| \cong 2.46$ Å e $\beta = 3eV$.

The three-dimensional representation of the dispersion relation, is shown in Fig.1.14 (a).

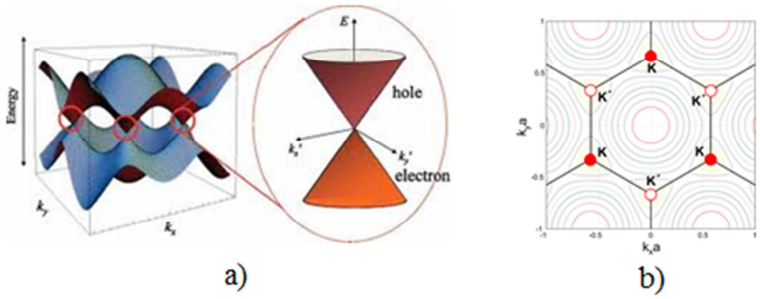

Fig.1.14: Dispersion diagram in graphene. a) Three-dimensional band structure of graphene. The conduction and valence band have contacts in the points K. b) Level lines of dispersion diagram. The hexagon formed by six points K defines the unit cell of graphene in the plane K. k_1 and k_2 are the only two non-equivalent K points that satisfy the condition = k_1=-k_2.

The band structure consists of two large "tents". The tent above represents the conduction band π*, the one lower the valence band π.

At the vertices of the hexagon, which represents the first Brillouin zone of graphene, the two bands are in contact at particular points.

These special points, where the conduction and valence band are degenerate[13], are called points *k*.

The valence band, corresponding to negative energies, is completely filled becouse the number of electrons equals the number of orbitals. The Fermi level [14]corresponds to the zero energy and therefore it coincides with the six points *k*. These points *k* are responsible of the electronic properties of graphene and of its *semimetal* behavior.

For the conductive properties of graphene are fundamental the energy states around the Fermi level. In fact, in this area, , the electronic states are located on the dispersion cones whose centers coincide with the points k as shown in Fig.1.15, [16].

[13] **Degenerate:** energy states with different quantum numbers but with the same energy are defined degenerate. The number of degenerate states is called degeneration.

[14] **Fermi level:** it is a hypothetical level of potential energy for an electron inside a crystalline solidis In details, it is the maximum energy of the electrons at T = 0 K and represents the energy level with probability 1/2 to be occupied by an electron at T = 0 K

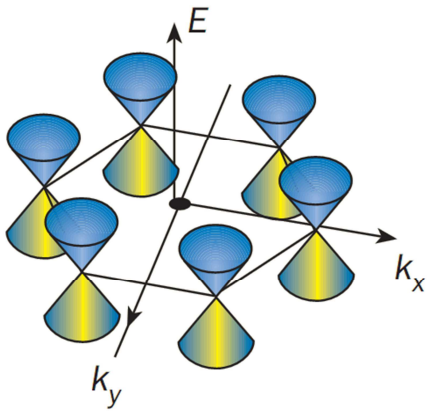

Fig.1.15: Approximated dispersion diagram around the points *k*.

Around these points, the electron hasn't the typical parabolic dispersion in a free space or in a material, $E = \hbar^2 k^2 / 2m^*$, but the dispersion becomes $E = \nu_F \hbar k$, where ν_F is the Fermi velocity of electrons in graphene. This relation is similar to that of massless particles like photons, for which $E = c\hbar k$, where *c* is the light speed.

So in the band π and π^*, near the points *k*, the electrons and holes in graphene behave more like massless quantum particles that as ones with mass. In this case electrons and holes are called *Dirac fermions* and *k* points are often called the *Dirac points* [17],[18].

It also possible to show that the slope of the cone is equal to$\frac{\sqrt{3}}{2} t_0 a$ where t_o=2.7eV [19].

The particular band structure of graphene is determined by the way in which electrons scatter on atoms of the crystal lattice. Its band diagram differs from the metal or the semiconducting ones, being in the middle between these.

In many directions, the electrons that propagate at the Fermi level are backscattered from atoms in the lattice leading to an energy band gap as in semiconductors. Instead, in the other directions, when the electrons are scattered in distructive manner such to remove the backscatter its behavior becomes metallic.

1.3.2 Electronic properties of SWCNTs

SWNTs can exhibit the metal or semiconductor behavior depending on how the graphene sheet is rolled to form the cylinder of the nanotube because this modifies the band diagram of graphene.

The direction of rolling and the diameter of the nanotube can be obtained from the pair of integers (n, m), which identify the type of tube.

All armchair SWCNT have metallic behavior; those with n-m = 3k, where $k \neq 0$, are semiconductors with a small band gap.

All the others are semiconductors with a band gap inversely proportional to the diameter of the nanotube.

To determine the Brillouin zone inherent the bi-dimensional unit cell of the CNT,defined by the chiral vector *C* and the translation vector *T*, we construct the corresponding vectors of the reciprocal lattice, *C** and *T**, respectively, parallel to *C* and *T* and having a length $\frac{2\pi}{|C|}$ and $\frac{2\pi}{|T|}$. The Brillouin zone of the CNT is given by the rectangle described by C* and T*.

When the bi-dimensional unit cell of the CNT is rolled, the electron is bound to moving in a periodic potential, with a period $C = |C|$.

This periodicity implies that, due the condition of stationarity of the wave associated with the electron, must be satisfied the following *quantization condition*:

$$C \cdot k = 2\pi q \quad \text{or equivalently} \quad |C| = \lambda q \qquad 1.11$$

where q is a not null integer and λ is the wavelength (De Broglie) associated with the electron.

The quantization condition leads to a discretization of energy levels along the circumference C, giving rise to a series of lines of quantization corresponding to the allowable values for the pairs (kx, ky): the component of k perpendicular to the axis of the CNT, $k_{\perp}$, can take discrete values , while the component of k parallel to axis of the CNT, $k_{/\!/}$, remains a continuous variable, as shown in Fig.1.16.

Therefore, the electrons are free to roam long distances in the direction of the length of the CNT.

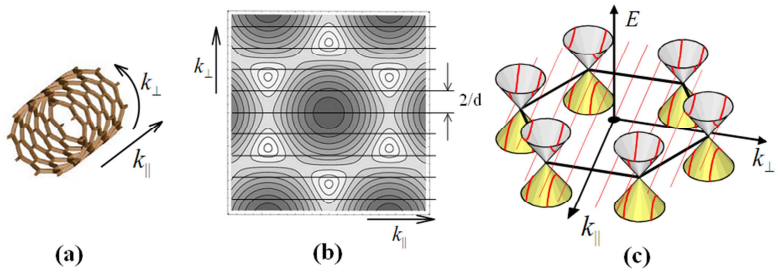

Fig.1.16: Quantization of the wavevectors in a CNT. a) The wavevector parallel and perpendicular to the axis of the CNT. b) Level lines of band diagram of a CNT with θ=0. The parallel lines spaced *2/d* are the wavevectors k permits. Each line is a 1D sub-band. c) Electronic states, near the Fermi level of the CNT, defined by the intersections of the allowed values of k with the band diagram of graphene in the points k.

The parallel lines in Fig.1.16 b) are the allowed states *k* in a CNT. The planes parallel to the y-axis (energy axis) pass through the quantization lines cutting the dispersion graph of graphene in slices, (Fig. 1.16c) which collected in a graph (E, $k_{/\!/}$) are the 1D sub-bands in the scatter plot of the CNT. In the space of reciprocal lattice, quantization lines are spaced by an amount equal to:

$$\Delta k = \frac{2\pi}{|C|} = \frac{2}{d} \qquad 1.12$$

depending exclusively on the diameter of the nanotube.

As anticipated, depending on the direction in which the graphene sheet is wrapped, is possible to identify CNTs of type of zig-zag, armchair or chiral.

In this case, change the intersections between the lines of the allowed wavevector k and cones of the dispersion diagram in the points *k*. For this reason, SWCNT may have different electrical characteristics [19].

In particular, if the CNT is wrapped around the x axis it is of armchair type and lines of quantized wavevector pass exactly for K1 (or K2). In this case, CNT present a metallic behavior, Fig.1.17 a).

Instead, if the CNT is wrapped around the y-axis is the CNT is of type zig-zag type and lines of quantized wavevector does not pass through any point *k*. Thus, in the dispersion diagram of CNT, will be a gap between the valence and conduction band and CNT will present a semiconductor behavior, Fig.1.17 b).

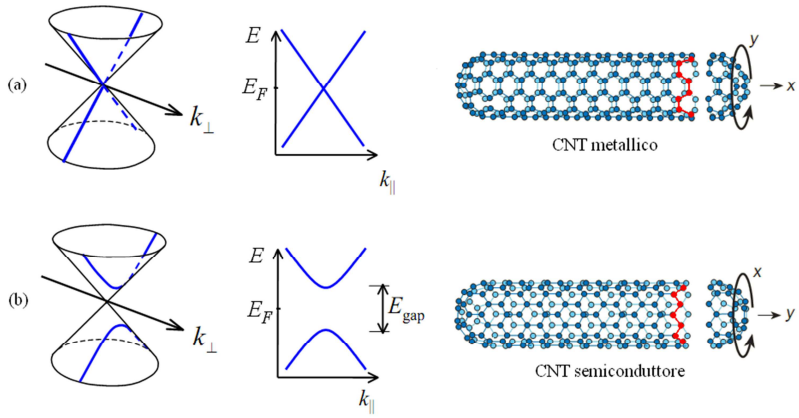

Fig.1.17: Different alignments between the cone of dispersion a K1 and lines of the quantized vector k. (a) The 1D sub-band nearest to the Fermi level passes through the point K1 and the CNT shows metallic behavior. (b) The 1D sub-band nearest to the Fermi level does not intercept the point K1, so a band gap is formed and the CNT shows a semiconductor behavior.

In mathematical terms, expressing the relationship that describes the quantization condition along the circumference as a function of k_x and k_y, we obtain:

$$(na_{1x} + ma_{2x})k_x + (na_{1y} + ma_{2y})k_y = 2\pi q \qquad 1.13$$

from which, substituting the expressions of a_1 and a_2 we obtain:

$$k_y = \frac{4\pi q}{3a_0(n+m)} - \frac{(-n+m)}{\sqrt{3}(n+m)}k_y \qquad 1.14$$

To understand the electronic properties of CNT is necessary to consider the number N of unit cells of graphene contained in the unit cell of the CNT previously introduced. This number is the ratio between the area of the unit cell of graphene and that of the unit cell of the CNT.

By imposing the initial condition C·T=0, developing the scalar product and remembering that t_1 and t_2 are prime numbers between them, we have:

$$T = \frac{a_1(2m+n) - a_2(m+2n)}{MCD\{(n+2m),(2n+m)\}} \quad 1.15$$

where MCD{a,b} indicates the greatest common divisor of a and b. The area of the unit cell of the CNT is:

$$A_{CNT} = |C \times T| = \frac{2|a_1 \times a_2|(m^2+nm+n^2)}{MCD\{(n+2m),(2n+m)\}} \quad 1.16$$

while the area of the cell of graphene corresponds to:

$$A_{GFR} = |a_1 \times a_2| = 3a_0^2 \sin\left(\frac{\pi}{3}\right) = 3\frac{\sqrt{3}}{2}a_0^2 \quad 1.17$$

from which is possible to obtain:

$$N = \frac{A_{CNT}}{A_{GFR}} = \frac{2(m^2+nm+n^2)}{MCD\{(n+2m),(2n+m)\}} \quad 1.18$$

The area of the unit cell of the nanotube is *N* times larger than that of the graphene sheet, so the area of the unit cell of the same in the reciprocal space is 1/*N* times smaller.

As function of *N*, some constraints on the integer *q* introduced in the quantization condition can be obtained. Rewriting the wavevector *k* as a function of C* and T* we obtain:

$$k = k_{C^*}C^* + k_{T^*}T^* \quad 1.19$$

with:

$$C^* = \frac{(-t_2 b_1 + t_1 b_2)}{N} \qquad T^* = \frac{(mb_1 - nb_2)}{N} \quad 1.20$$

the quantization condition can be reformulated as $kC^* = q$. Therefore, to avoid the degeneracy condition must be $0 \leq q \leq N-1$.

This means that there are *N* discrete values of *k* in the direction of the chiral vector.

1.3.3 Electronic properties of MWCNTs

SWCNTs behave as quantum wires, i.e. 1D conductors. Since in these conductors the Coulomb interaction between the electrons is not well shielded, is present a gas of correlated electrons, called *Luttinger liquid* [15][20]. Since the MWCNTs consisting of more SWCNTs, one might think that they have electronic properties of 2D conductors, but is still observed electronic behavior of Luttinger liquid type. Due to the weak interaction between the first layers neighbors, the MWCNTs have a band structure much more complex than that of SWCNTs and graphite.

These nanotubes show intermediate characteristics between those of SWCNT and those of graphite, and for this reason are called *mesoscopic*. Generally, the following conditions are true:

- if the diameter of MWCNT is much greater than the mean free path, $d >> \lambda_{mfp}$, the electronic transport is of 2D diffusive type and the density of states is similar to that of graphene without singularity of Van Hove;

[15] **Luttinger liquid:** A Tomonaga-Luttinger liquid, more often referred to as simply a Luttinger liquid, is a theoretical model describing interacting electrons (or other fermions) in a one-dimensional conductor (e.g. quantum wires such as carbon nanotubes). Such a model is necessary as the commonly used Fermi liquid model breaks down for one dimension. The Tomonaga-Luttinger liquid was first proposed by Tomonaga in 1950. The model showed that under certain constraints, second-order interactions between electrons could be modelled as bosonic interactions. In 1963, Luttinger reformulated the theory in terms of Bloch sound waves and showed that the constraints proposed by Tomonaga were unnecessary in order to treat the second-order perturbations as bosons. But his solution of the model was incorrect, the correct one was given by Mattis and Lieb 1965. Among the hallmark features of a Luttinger liquid are the following:
-Likewise, there are spin density waves (whose velocity, to lowest approximation, is equal to the unperturbed Fermi velocity). These propagate independently from the charge density waves. This fact is known as spin-charge separation.
-Charge and spin waves are the elementary excitations of the Luttinger liquid, unlike the quasiparticles of the Fermi liquid (which carry both spin and charge). The mathematical description becomes very simple in terms of these waves (solving the one-dimensional wave equation), and most of the work consists in transforming back to obtain the properties of the particles themselves (or treating impurities and other situations where 'backscattering' is important). See bosonization for one technique used.
- Even at zero temperature, the particles' momentum distribution function does not display a sharp jump, in contrast to the Fermi liquid (where this jump indicates the Fermi surface).
-There is no 'quasiparticle peak' in the momentum-dependent spectral function (i.e. no peak whose width becomes much smaller than the excitation energy above the Fermi level, as is the case for the Fermi liquid). Instead, there is a power-law singularity, with a 'non-universal' exponent that depends on the interaction strength.

- if the diameter of the MWCNT is comparable with the mean free path, $d \approx \lambda_{mfp}$, transport is not completely 2D diffusive but not even 1D ballistic

For better clarity on the electronic properties of MWCNTs is convenient to consider only two weakly coupled tubes into one another. For these configurations:

- if a tube is semiconductor and the other is metallic, the electronic properties for low energies (around the Fermi level) are determined by the metallic tube and there aren't variations in the DOS around the Fermi level;
- if both tubes are metallic, the situation is more complicated. In fact, if a tube is of type armchair and the other of type zig-zag, due to overlap of the energy bands in different points K, the hybridization is very weak around the Fermi energy and the density of states is the sum of the two. Instead, in the case in which the two tubes have the same chirality, there is a considerable variation in band structure.

These approximations are not valid for two strongly coupled or doped nanotubes and the Fermi level shifts in the valence band or in the conduction one [21].

Unlike SWCNTs that can be either metallic or semiconductor depending on their chirality, MWCNTs are always metallic with a current carry capability similar to the metallic SWCNTs. Initially, several experiments indicated that the conduction was due exclusively to the outer shell in an MWCNT. Later it was confirmed that in reality, if suitably connected, all the shells take part in the conduction phenomenon [22].

Due to the large diameter, all the shells of a MWCNTs are conductive even if according to the chirality are semiconductors. This can be explained by considering the band structure of a nanotube of large diameter [23]. Fig.1.18(a) shows the band structure of a shell of zig-zag type with a diameter of 20 nm and chiral indices (256.0). In Fig.1.18(b) is reported a zoom around the Fermi level and each line denotes a sub-band of the CNT.

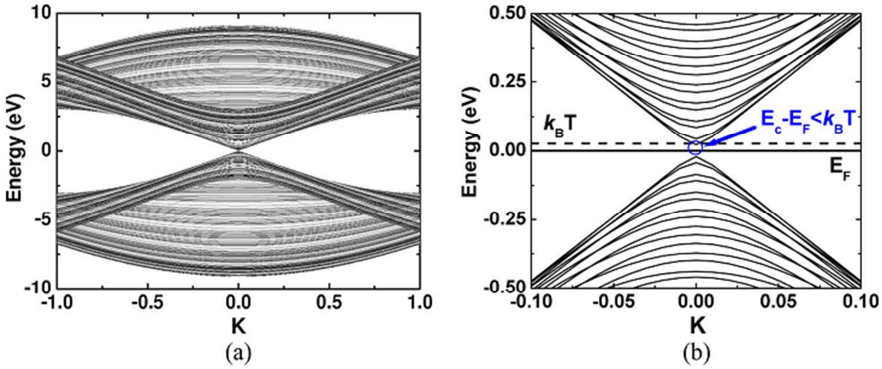

Fig.1.18: (a):Band structure of a zig-zag SWCNT (256.0); (b): Zoom of the band structure around k = 0.

From the figure above is possible to observe the presence of a band-gap which confirms that the CNT is semiconductor. At room temperature (T=300K), the thermal energy k_BT is equal approximately to 0.0258 eV, where k_B is the Boltzmann constant.

Fig.1.18 (b) highlights that the difference of energy between the edge of the conduction band E_C and the Fermi level E_F is less than 0.0258 eV. Therefore when the diameter of a CNT is around 20nm or higher, the band-gap will be exceeded by the room temperature.

Furthermore, even if the difference of energy between the sub-bands and E_F is greater than k_BT, this difference of energy is relatively small thanks to the high density of states in the shell with large diameter.

In these sub-bands, the electrons have a high probability of appearing f_i at E_F according to the Fermi-Dirac distribution function[16]:

[16] **Fermi-Dirac distribution function:** is a part of the science of physics that describes the energies of single particles in a system comprising many identical particles that obey the Pauli Exclusion Principle. It is named after Enrico Fermi and Paul Dirac, who each discovered it independently. Fermi–Dirac (F–D) statistics applies to identical particles with half-odd-integer spin in a system in thermal equilibrium. Additionally, the particles in this system are assumed to have negligible mutual interaction. This allows the many-particle system to be described in terms of single-particle energy states. The result is the F–D distribution of particles over these states and includes the condition that no two particles can occupy the same state, which has a considerable effect on the properties of the system. Since F–D statistics applies to particles with half-integer spin, they have come to be called fermions. It is most commonly applied to electrons, which are fermions with spin 1/2. Fermi–Dirac statistics is a part of the more general field of statistical mechanics and uses the principles of quantum mechanics

$$f_i = \frac{1}{exp\left(\frac{|E_i - E_F|}{K_{BT}}\right) + 1} \qquad 1.21$$

where E_i is the largest (or smallest) energy for the sub-bands below (or above) the Fermi level E_F. Since there are a large number of sub-bands in the shell with large diameter, their cumulative effect on the probability may be large, which implies that can have a lot of conductive channels

Generally the following condition is satisfied : for MWCNTs of length below a critical threshold (typically around the 7μm) the conductivity decreases with increasing of the diameter, while for MWCNTs longer than this value the increase in the diameter leads to an increase of the conductivity.

Potentially, for lengths of the order of hundreds of μm, the conductivity of MWCNTs can be several times higher than that of copper and SWCNT bundles.

For short lengths (<10μm) the bundles of SWCNT show a conductivity more than two times greater than that of MWCNTs.

1.3.4 Conductance of CNT

In the case of CNT since its diameter is much smaller than the *mean free path* [17](mfp) of the electron, d < λmfp, it is possible the occurence of 1D *ballistic conduction*, i.e. the electrons cross the CNT without undergoing scattering and therefore without heat the nanotube. Due to this property, CNTs are of particular interest as nanoscale interconnects.

Both SWCNT that MWCNTs behave as quantum wires due to the effect of confinement on the circumference of the CNT, [24],[25].

The conductance of a SWCNT or MWCNT is given by:

1.22

[17] **Mean Free Path:** In physics, it is the average distance covered by a moving particle (such as an atom, a molecule, a photon) between successive impacts (collisions) which modify its direction or energy or other particle properties.

$$G = G_0 M = \frac{2e^2}{h} M$$

where:

- G_0=2e^2/h=(12.9kΩ)$^{-1}$ is the conductance quantum;
- h=6.62·10^{-34}Js is the Plank's costant;
- M is the apparent number of conductive channels (M = 2 for a SWNT without defects).

However, *M*, is determined not only by the intrinsic properties of a nanotube, but also from defects, impurities, structural distortions, coupling with the substrate and contacts.

Consequently, the conductance measured experimentally is much lower of the quantized value.

The measured resistance for a SWCNT is ~10kΩ, in comparison with the value perfect of 12.9 /2= 6.45 kΩ.

1.4 Carbon nanotube: other properties

Interest in carbon nanotubes is due to the fact that they have unique mechanical, thermal, electrochemical and electronic properties, in part derived from the similarity with the graphite, but in large part due to the CNTs as nano-structures.

In Table 1 the relevant properties of CNTs are shown and compared with those of materials currently used in various electronic and industrial applications [13,17].

Table 1. 1 Comparison of properties: CNT-Materials currently used

PROPERTY	CNT	COMPARISON
Dimension	0.6 – 2nm (SWNT) 0.6 – 100nm (MWNT)	Si: at least 50 nm
Current density	Semiconductor o metal $>10^{9}$ A/cm^{2}	Cu: 10^{6} A/cm^{2}
Field emission	1-3 kV/µm da singolo CNT	Mo: 50 – 100 kV/µm
Thermal conductivity	6000 W/m•K	Diamond 3320 W/m•K
Density	1.4 g/cm^{3}	Al: 2.7 g/cm^{3}
Tensile strength	~ 75 GPa (SWCNT) ~ 150 GPa(MWNT)	Steel: 2 GPa with density from 3 to 6 times higher
Young's modulus	1054 GPa (SWCNT) 1200 GPa (MWCNT)	Steel: 208 GPa
Cost	1500 $/g	Au 10 /g

Since the sp^2 bonds in the CNT and graphene are very strong, these materials are the more resistant ever measured. CNTs have also a high current carrying capability, at least two orders of magnitude greater than that of copper. In addition, CNTs have a mean free path [18](of the order of um) much greater than the classical conductors (Cu:40nm) due to the weak scattering with acoustic phonons and the absence of scattering with optical phonons at room temperature [26]. Due to the high aspect ratio (length divided the diameter), CNTs can be

[18] **Mean free path:** in physics, the mean free path is the average distance covered by a moving particle (such as an atom, a molecule, a photon, electron) between successive impacts (collisions) which modify its direction or energy or other particle properties.

considered as quantum-wires[19], ie a 1D system in which the conduction is longitudinal and not transversely.

These important properties such as the high form factor (ratio between the length *L* and diameter *d*), the electronic transport properties (mean free path of the order of um), the high value of Young's modulus, the high thermal and electrical conductivity have stimulated a strong interest of scientific research aimed at developing new composites with specific electromagnetic properties.

All these factors make nanotubes an excellent candidate for the development of nanostructured materials for a wide variety of applications.

Typically important uses are for example as antistatic elements, electrostatic dissipative ones or for electromagnetic shielding in the field of the aeronautic, automotive and electronic industries.

Despite intensive research efforts devoted to them since their discovery, their applications and methods of use for maximum benefit, have not yet been studied exhaustively.
Some of these properties will be discussed in the next paragraphs.

1.4.1 Mechanical properties

Carbon nanotubes have a strong mechanical resistance that for a material depends on several factors including the strength of atom-atom bonds in the lattice and the absence of structural defects in the same.

The presence of defects is very important in breaking strength of a material, because to break a material free from defects is necessary to

---

[19] **Quantum-Wire:** in condensed matter physics, a quantum wire is an electrically conducting wire, in which quantum effects are affecting transport properties. Due to the quantum confinement of conduction electrons in the transverse direction of the wire, their transverse energy is quantized into a series of discrete values E0 ("ground state" energy, with lower value), E1. One consequence of this quantization is that the classical formula for calculating the electrical resistivity of a wire: $R=\rho\cdot(l/A)$ is not valid for quantum wires (where ρ is the resistivity, l is the length, and A is the cross-sectional area of the wire). Instead, an exact calculation of the transverse energies of the confined electrons has to be performed to calculate a wire's resistance. Following from the quantization of electron energy, the resistance is also found to be quantized. The importance of the quantization is inversely proportional to the diameter of the nanowire for a given material. From material to material, it is dependent on the electronic properties, especially on the effective mass of the electrons. In simple words, it means that it will depend on how conduction electrons interact with the atoms within a given material.

break all the bonds that compose it. So the presence of defects reduces the tensile strength.

Ideally, the tension that can be supported by a CNT is comparable to the tensile strength of the C-C bond in a benzene ring. For this reason, CNTs are the strongest material ever found.

Just to give an idea, the tensile strength predicted theoretically for Kevlar, a synthetic fiber whose main feature is the great mechanical resistance is 29.6 GPa, while that of an armchair SWCNT reaches 126.2 GPa.

In addition CNTs are also flexible material: they can be folded up to about 90 degrees without breaking (see Fig.1.19), [27].

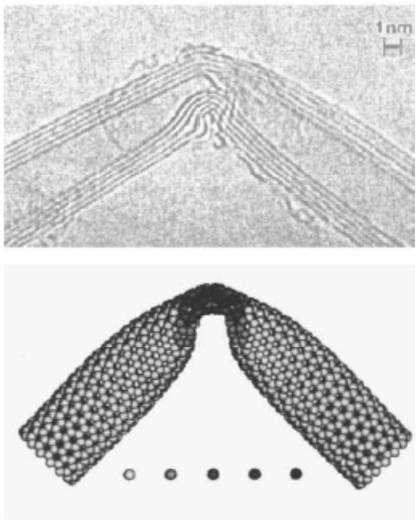

Fig.1.19: Experimental result (up) and simulation (down) of a large-amplitude transverse deformation of a carbon nanotube, apparently beyond the elastic limit, [27].

The deformations also affect the electronic properties of nanotubes, especially metal ones, changing their band-gap (Fig.1.20),[28].

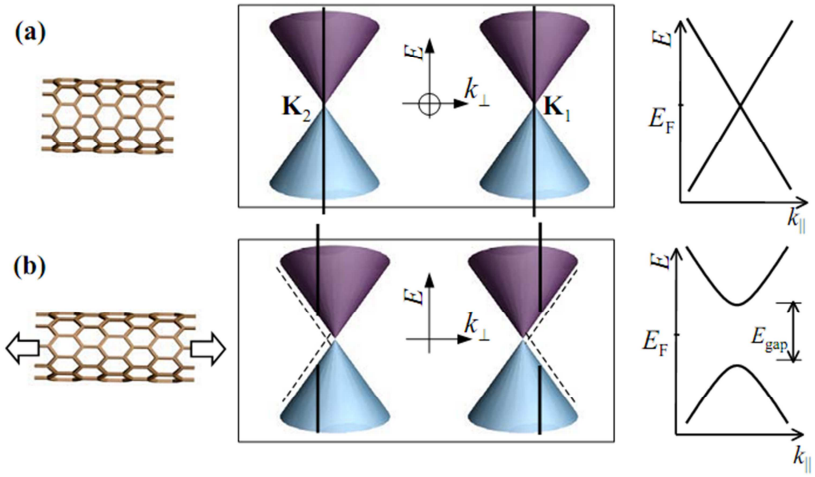

Fig.1.20: Effect of stretching on the band-gap of a zigzag SWCNT. The quantized values of $k_\perp$ are represented by vertical lines that intercept the centers of the cones in the points K1 and K2. (a) The allowed **k** intercept the points K and 1D sub-bands near K_1 and K_2 have zero band-gap. (b) At the points K, the quantized values $k_\perp$ deviate when the CNT is in tension and opens a band-gap in 1D sub-bands.

A armchair SWCNT intrinsically metallic, is characterized by the opening of a band-gap in the presence of torsion.

A metallic tube of zig-zag type, instead, is characterized by the opening of a band-gap in the presence of tension.

Finally a chiral metallic tube becomes semiconductor in the presence of both types of deformation.

1.4.2 Thermal properties

The value of the thermal conductivity, at room temperature, for a SWCNT, estimated by means of molecular dynamics calculations, is about 6600 W/m·K [29]. Therefore it is higher than that of pure diamond (3320 W/m·K), material with exceptional thermal conductivity, with a value five times higher than that of Copper.

This means that, at least in theory, the SWCNT can be defined as the best conductor of heat that exists in nature. Unlike metals, for

which the thermal energy is transmitted mainly by the electrons, thermal conductivity of carbon nanotube systems are determined mainly by phonons and at low temperatures is dominated by acoustic phonons. In more detail, the thermal conductivity is proportional to the product of specific heat for the speed of sound and for the phonon mean free path.

Since SWCNTs are characterized by a long phonon mean free path (due to the absence of defects at the atomic scale), a high speed of transmission of sound (~ 10^4m/s) and a high specific heat, the high calculated conductivity values are expected.

Experimental measurements were performed with different methodologies and the results show, that generally, the value of the thermal conductivity decreases when the nanotubes are aggregated in bundles, perhaps due to the decrease of the phonon mean free path [30], [31].

For this interesting property, the nanotubes could be integrated successfully in microelectronic devices, where exploiting the anisotropic properties of conduction and rapid heat dispersion of the tubes, the exercise time of the apparatuses can increase considerably.

1.4.3 Chemical and electrochemical properties

Due to their tubular shape, the nanotubes show of the strong properties of capillarity [32] that together with the high surface / weight ratio, makes them ideal materials for the adsorption of liquids and gases. The properties of adsorption of the nanotubes have been studied especially in the case of the adsorption of Hydrogen, in view of a its possible use in fuel cells.

Infact, all systems up to now used for storage (cylinders, hydrides, active carbons) require to work at high pressure and low temperature to be able to store a sufficient amount of gas.

However, many research efforts must be concentrated in this area to exploit nanotubes for this purpose [33].

Carbon nanotubes find also applications as electrodes of supercapacitors (or electrochemical capacitors), i.e. accumulators capable of storing large amounts of energy and characterized by processes of charge and discharge very fast. These properties are due

to high porosity and, therefore, to the high effective surface area with which are characterized the electrodes of such devices.

The nanotubes show themselves ideal candidates for this type of application considered their high surface area, estimated at ~ 1300 m^2/g.

Considered that the conductivity of the nanotubes depends strongly by their structure, from a possible doping and by the environmental conditions, it is possible to use them also as chemical sensors.

Sensors based on nanotubes, able to respond to the absorption of some gaseous species (among which especially NO_2 and NH_3) in terms of variations of electrical conductivity, have been realized. The advantages of these sensors, compared to the traditional ones, are the possibility of obtaining selective systems, reversible and able to operate at room temperature with response times very quick.

Sensors and biosensors CNT-based have been assembled with success for the electrochemical determination of several chemical species of biological and environmental interest (such as glucose, serotonin, epinephrine, ascorbic acid, uric acid, etc). These sensors contain an electrochemical activity and a generally higher sensitivity compared to traditional graphite electrodes. In addition they are chemically inert and of reduced size.

References

[1] S. Ijima. “Helical microtubules of graphitic carbon", Nature 354, pp56-8, 1991.

[2] Lide, D. R., ed (2005). CRC Handbook of Chemistry and Physics (86th ed.). Boca Raton (FL): CRC Press. ISBN 0-8493-0486-5.

[3] P. Delhaes (2001). Graphite and Precursors. CRC Press. ISBN 9056992287

[4] N Deprez and D S McLachlan “The analysis of the electrical conductivity of graphite conductivity of graphite powders during compaction” 1988 J. Phys. D: Appl. Phys. 21 101 doi:10.1088/0022-3727/21/1/015

[5] A.M. Rao, M.S. Dresselhaus, “Nanostructured form of Carbon: an overview”, Kluwer Academic, Erice, Italy (2000)
[6] M. Buongiorno-Nardelli, C.Brabec: "Lip-lip interaction and the growth of multi-walled carbon nanotubes" - Phys. Rev. Lett. 80, 313 (1998).
[7] P. Ciambelli, D. Sannino, M. Sarno, C. Leone, U. Lafont, "Effects of alumina phases and process parameters on the carbon nanotubes growth", Diam. Relat. Mater. 16, pp.1144-1149, 2007.
[8] D. S. Bethune, C. H. Klang, M. S. D. Vries, G. Gorman, others: "Cobalt catalyzed growth of carbon nanotubes" - Nature 363, 605 (1993).
[9] M. S. Dresselhaus, G. Dresselhaus, Ph. Avouirs. Carbon Nantubes, Topics Appl. Physics. SPIN Springer's internal project, 2000.
[10] G. W. Hanson. “Fundamentals of Nanoelectronics”. Pearson Prentice Hall, 2008.
[11] L. Guadagno, B. De Vivo, A. Di Bartolomeo, P. Lamberti, A. Sorrentino, V. Tucci, L. Vertuccio, V. Vittoria “Effect of functionalization on the thermo-mechanical and electrical behavior of multi-wall carbon nanotube/epoxy composites”, Carbon 49 (2011), pp 1919-1930.
[12] Wikipedia: The Free Encyclopedia
[13] R. Saito, G. Dresselhaus, S. Dresselhaus. Physical Properties of Carbon Nantubes. London, U. K.: Imperial College Press, 1998.
[14] E. D. Minot. Tuning the band structure of carbon nanotubes. PhD thesis, Cornell University (USA), 2004.
[15] A. G. Perri, A. Giorgio. “I nanotubi di carbonio: caratterizzazione delle proprietà elettroniche ed applicazioni". La comunicazione, 2005. Politecnico di Bari (Italy).
[16] P. L. McEuen. “Single Wall Carbon Nanotubes". Physics Word, pages 31-36, June 2000.
[17] H. Li, C. Xu, N. Srivastava, K. Banerjee. “Carbon Nanomaterials for Next-Generation interconnects and Passives: Physics, Status and Prospects ". IEEE Trans. on Electron Devices, 56(9):1799-821, 2009
[18] G. W. Hanson. “Fundamentals of Nanoelectronics”. Pearson Prentice Hall, 2008.
[19] E. D. Minot, “Tuning the band structure of carbon nanotubes” PhD thesis, Cornell University (USA), 2004.

[20] P. J. Burke. “Luttinger liquid theory as a model of the gigahertz electrical properties of carbon nanotubes". IEEE Trans. On Nanotechnology, 1(3):129-44, 2002.

[21]Ph. Lambin, V. Meunier, A. Rubio, “Science and Application of Nanotubes”, D.Tománek, R.J. Enbody (Eds), Kluwer Academic/Plenum Publishers, New York, 17 (1999).

[22]A.Naeemi, J. D. Meindl, “Compact Physical Models for Multiwall Carbon-Nanotube Interconnects". IEEE Electron Device Letters, 27(5):338-40, 2006.

[23]H.Li, W. Yin, K. Banerjee, J. Mao,”Circuit Modeling and Performance Analysis of Multi-Walled Carbon Nanotube Interconnects" IEEE Trans. on Electron Device, 55(6):1328-36, 2008.

[24]M. Bockrath, D. H. Cobden, P. L. McEuen, N. G. Chopra, A. Zettl, A. Thess, R. E. Smalley, “Single-Electron Transport in Ropes of Carbon Nanotubes”, Science, Vol. 275, pp. 1922-1925, 1997.

[25]S. Frank, P. Poncharal, Z. L. Wang, W. A. de Heer, “Carbon Nanotube Quantum Resistors”, Science, Vol. 280, pp. 1744-1746, 1998.

[26] P.G. Collins, P. Avouris: “Nanotubes for electronics” – Scientific American 69, 2000.

[27] E. T. Thostenson, Z. Ren, Tsu-Wei Chou,” Advances in the science and technology of carbon nanotubes and their composites: a review”, Composites Science and. Technology, 61 pp.1899–1912, 2001.

[28] E. D. Minot, “Tuning the band structure of carbon nanotubes” PhD thesis, Cornell University (USA), 2004.

[29] F. Wu, X. He, Y. Zeng and H.-M. Cheng, “Thermal transport enhancement of multi-walled carbon nanotubes/ high-density polyethylene composites”, Applied Physics A: Materials Science & Processing, Vol. 85, N°1, pp. 25-28, 2006.

[30] Z. Shi, Y. Lian, F. Liao, X. Zhou, Z. Gu, Y. Zhang, S. Iijima, “Purification of single-wall carbon nanotubes”, Solid State Communications 112, pp. 35-37, 1999.

[31] J. Moon, K. Hyeok, Y.H. Lee, Y.S. Park, D.J. Bae, G. Park, J. Phys. Chem. B 105 (2001) 5677

[32] M.R. Pederson, J.Q. Broughton, “ Nanocapillarity in fullerene tubules”, Phys. Rev. Lett. 69, pp. 2689−2692, 1992.

[33]R.H. Baughman, A.A. Zakhidov, W.A. de Heer,“Carbon Nanotubes–The Route Towards Applications”, Science 297, pp. 787-792,2000

Chapter 2

Nanocomposites

The preparation of advanced nanostructured composites is currently required in several sectors and for various applications. This chapter is devoted to illustrate the advantages of nanocomposites as compared to classical materials.
A very important class of nanocomposites, on which this PhD work has been focused, can be obtained by using epoxy systems as matrix and either Carbon NanoTubes (CNTs) or CNTs-clay as fillers.

2.1 Introduction

Composite materials is a system composed of a combination of two or more constituents, different in form and chemical composition, that are essentially insoluble one in the other.

Instead, nanocomposites or nanostructured materials are a particular and new class of composite in which a component has at least one dimension of the order of nm.

The interest and the scientific importance of the topic is justified by the fact that the conventional materials haven't the suitable properties to satisfy the specific requirements for modern applications while two or more distinct materials are combined to form a material which possesses superior properties, or in any way relevant, with respect to properties of individual components.

In fact, the enormous use of composites materials is justified by their extraordinary combination of properties [1], low weight and ease of processing.

Thus the individuation and preparation of advanced composites with best features respect to the traditional materials is currently required in several industrial sectors, Fig.2.1, [2].

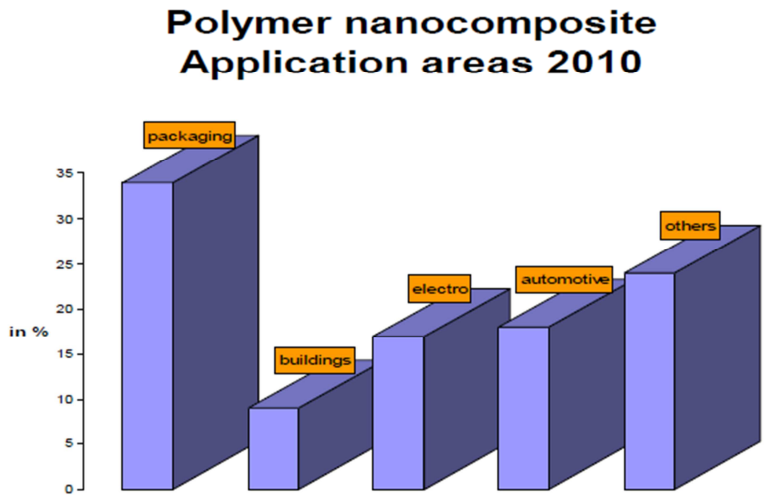

Fig.2.1: Polymer nanocomposite application. Font:Nanocomposite a global strategic business report, February 2011, Global Industry Analyst Inc.

Composite materials are orthotropic[20] and biphasic (i.e. consisting of two solid phases), one with a reinforcing function (fibers or charge) and one with binder task (matrix) [3].

The set of these two parts makes a product able to guarantee very high mechanical properties (fundamental is the interfacial adhesion between fibers and matrix) with lower density: for this reason the composites are widely used in applications where lightness is crucial, aircraft in the first place.

Do not forget that the use of composites has ancient origins. The first composites, obtained by mixing straw and clay (or mud), were

[20] **Orthotropic:** an orthotropic material has two or three mutually orthogonal twofold axes of rotational symmetry so that its mechanical properties are, in general, different along each axis. Orthotropic materials are thus anisotropic; their properties depend on the direction in which they are measured. An isotropic material, in contrast, has the same properties in every direction. One common example of an orthotropic material with two axis of symmetry would be a polymer reinforced by parallel glass or graphite fibers. The strength and stiffness of such a composite material will usually be greater in a direction parallel to the fibers than in the transverse direction.

used for the production of bricks for building construction: the straw was the reinforcement while the clay or mud, constituted the matrix.

Even in nature we can find exceptional examples of composite materials. The wood is a brilliant example, formed by a cellulose fibers reinforcement, mainly oriented in the longitudinal direction, contained in a lignin matrix. This strongly oriented arrangement of such fibers leads to high anisotropy of the mechanical characteristics of the wood in the different stress directions.

Among natural composites we can include also the bones, whose basic structure is composed of a network of collagen, which forms the reinforcement, embedded in a matrix of calcium, sodium, phosphorus, magnesium and fluoride. Both materials contribute to characterize the mechanical behavior of the bones, since the collagen fibers are resistant to tensile loads, while the matrix is resistant to compressive ones.

In any case, composite materials, are mainly designed to improve the following properties:

- *rigidity*: if high enough, it is possible to replace metal parts with polymer composite, much lighter, cheaper and easier to work;
- *electrical conductivity*: typically polymers are insulators but under suitable conditions they may exhibit a reversal of the electrical behavior from insulator to conductive.
- *flame resistance*, which is a major limitation of polymers;
- *resistance to chemicals* such as acids, bases, oils and weathering, due to the high permeability to small molecules;

2.2 Classification of nanocomposites

There are several methods for classifying composite materials. A first method catalogs the composites according to the type of matrix.

With this logic, the composites are distinguished into:

- *PMC (Polymer-Matrix Composite):* for example, thermoplastics[21] (such as Nylon) or thermosetting[22] (such as epoxy resins);
- *MMC (Metallic-Matrix Composite):* usually aluminum, or titanium and their alloys, more rarely, magnesium or others*;*
- *CMC (Ceramic-Matrix Composite):* generally of silicon carbide or alumina;

  In the first two types of composites (metallic and polymeric), being the matrix itself ductile, the task of the filler is usually to confer rigidity to the final material, as well as specific characteristics depending on the particular application.

Instead, in the ceramic matrix composites, being this generally brittle, the task of the filler is to increase the toughness, which however remains substantially low.

The composites studied in this activity are of polymeric type and therefore they will be further investigated in the following paragraphs.

Independently, in each of the systems presented above the matrix constitutes a continuous phase throughout the component. The union of two or more components (reinforcement and matrix) must necessarily give rise to a continuous solid material, which is capable of transmitting and redistribute the internal stresses, due to external stresses on its components.

Thus a further classification can be conducted on the basis of continuity:

- *Composite materials with continuous components* (both matrix and fiber);

---

[21] **Thermoplastic:** also known as a thermosoftening plastic, is a polymer that turns to a liquid when heated and freezes to a very glassy state when cooled sufficiently. This process, theoretically, may be repeated several times according to the quality of different plastics.

[22] **Thermosettings:** also known as a thermoset, are polymer materials which, after an initial phase of softening due to heating, harden as result of three-dimensional reticulation. In the phase of softening through the combined effect of heat and pressure are moldable. If these materials are heated after hardening does not return workable, but they decompose

- *Composite materials with two components,* one of which is continuous and the other discontinuous;
- *Multi-component materials,* some of which are continuous and other discontinuous

Generally, the composites that find application in the aircraft field belong to the last group.

Another classification is based on the dimensional morphology of nanomaterials used in the composite.

Terminology issues were solved recently with ISO[23] standardization also to avoid ambiguities and inconsistencies regarding this classification.

Thus, a standardization committee, ISO TC229 "Nanotechnologies", started in 2005, produced a set of documents (ISO/TS27687-2008, ISO/TS11360-2010, ISO/TS88004-2011) that list unambiguous terms and definitions related to particles in the field of nanotechnologies, limiting confusion in their indication [4].

Therefore, it is intended to facilitate communications between organizations and individuals in industry and those who interact with them.

According to such standardization, nanocomposites are considered as one family of nanomaterials, where a nano-object is dispersed into a matrix or a phase. The other families are mainly nanostructured materials in surface, multi-layer or volume.

A nanocomposite is a multiphase solid material where one of the phases has one, two or three dimensions of less than 100 nm [5].

The nanocomposites can be distributed according to the nanofillers, as classified in reference ISO/TS27687-2008 and highlighted in Fig.2.2.

[23] **ISO:** The International Organization for Standardization, widely known as ISO, is an international standard-setting body composed of representatives from various national standards organizations. Founded on February 23, 1947, the organization promulgates worldwide proprietary, industrial and commercial standards. It has its headquarters in Geneva, Switzerland.

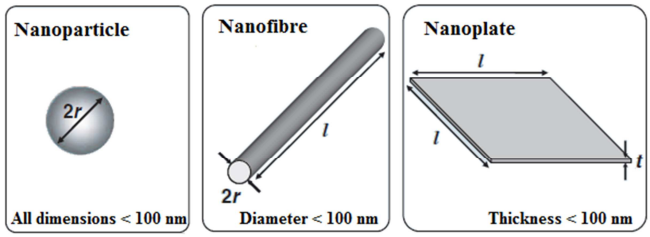

Fig.2.2: Nano-objects used for nanocomposites, as defined in ISO/TS27687 (2008)

A nanocomposite is a multiphase solid material where one of the phases has one, two or three dimensions of less than 100 nm [5]:

- *One-dimensional nanofiller:* in the form of plates, laminas and/or shells;
- *Two-dimensional nanofiller*: nanotubes and nanofibres which diameter is lower than 0.1 μm;
- Three-dimensional nanofiller: isodimensional nanoparticles such as nanometric silica beads.

The use of nanofillers allows to achieve a their good dispersion in the polymer. In this way it is possible to obtain mechanical, thermal, optical and chemical-physical properties, considerably higher compared to conventional composites [6]. Even at low contents of nanofillers (less than 5% in weight) there is a significant quality improvement in most of the properties [7].

2.3 Polymer-matrix composites (PMC)

The term polymer-matrix nanocomposite denotes a multicomponent system in which the material present in greater amount is constituted by a polymer, or a mixture of polymers, while the minority constituent is given by a material that has a size which is at least below 100 nm.

These matrices can be divided, according to their workability, in thermosetting matrices (TI) and thermoplastic ones (TP).

The TI matrices are characterized by a high "wettability" in the sense that blend easily with the fibers. The chemical bond is very strong and ensures continuity in the composite.

Instead, the TP matrices, being viscous fluids, require high operating pressures during processing. This requires a more complex technological system as well as a high cost. The bond with the fibers is not of a chemical type, but mechanical. It stems from a compressive hyperstatic stress state on the boundary, due to the different thermal expansion coefficient during the cooling.

Among the TI resins are widely used the polyester and the epoxy ones, both of organic type.

The polyester resins have low costs and low performances and are usually used with glass fibers, which are also of low cost, to form a composite called "*fiberglass*", much used in the production of boats.

Such resins polymerize very easily and in short times, even at room temperature, and therefore can be used for fast and economic works. As concerns their performance, this resins have discrete mechanical characteristics up to 250 ° C, are flame resistant and have good dielectric properties[8].

Summarizing, PMC are very popular due these following properties:

- High tensile strength;
- High stiffness;
- High Fracture Toughness;
- Good abrasion resistance;
- Good corrosion resistance;
- Low cost.

Properties of Polymer Matrix Composites are determined by:

- Properties of the fibers;
- Orientation of the fibers;
- Concentration of the fibers;
- Properties of the matrix.

Polymer Matrix Composites (PMC) are mainly used for manufacturing: aerospace structures, , automotive parts (brake and clutch linings), radio controlled vehicles, sport goods (skis, tennis racquets, fishing rods), etc.

2.3.1 The epoxy resin

Introduced on the market in the late ‘40, these thermosetting resins have a remarkable combination of properties such as excellent adhesion to the fibers, good chemical resistance, a greater mechanical strength compared to polyester resins and good thermal insulation properties [9].

In fact, the epoxy resins are suitable to work at temperatures up to 150 ° C and if realized with suitable additives, even up to 200 °C [10].

For these interesting properties they have found wide application in many fields ranging from advanced aerospace systems to commodity plastics.Except for some special types, pure resins do not found applications but require addition of chemical compounds called "*hardener*" to be transformed into rigid structural materials (curing[24]).

The "*curing agents*" usable for epoxy resins are many and their reactions with the resins are varied and complex. In general they occur without the liberation of volatile substances and with minimum volume change.

The epoxy resins are characterized by a molecule containing two or more epoxy reactive groups, usually located at the end of chain.

The number of this groups in each chain determines the functionality of the resin, which influence the reactivity during the curing process. The chemical symbol of an epoxy group is represented in Fig.2.3.

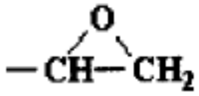

Fig.2. 3: Epoxy group

The low molecular weight of the uncured epoxy resins and in the liquid state gives them exceptionally high molecular mobility during processing. This property allows the liquid epoxy resin to wet the surfaces quickly and completely. The wetting properties are important when the epoxy resins are used in reinforced materials and as adhesives.

[24] **Curing:** is the set of reactions which leads to hardening of the epoxy resin, in a range of appropriate temperature; the process can take minutes to hours

Acting on the formulation of the reaction blend, i.e. modifying the content of epoxy resin, the curing agents and any fillers, it is possible to vary and balance the properties of the resin, in order to obtain a specific material for a particular use.

In fact, the chemistry of epoxies allows to produce cure polymers with a very broad range of properties.

For example, although epoxy resins are typically electrically insulating, many their properties can be modified with the addition of CNT, obtaining (for a phenomenon which will be illustrated in the next part) thermal conductivity combined with good electrical conductivity for several applications.

In this context, the use of multi-walled carbon nanotubes rather than single wall type is justified by two simple reasons. The first is that the MWCNTs are obtained with a manufacturing process much simpler than that required for the production of SWCNTs and this means at a lower cost

The second reason is that it is required the use of conductive filler and the SWCNT can be only partially (about 33%) on the total used concentration. Moreover, the precise knowledge of this content is indispensable for a correct characterization of the material.

2.4 Interface area with filler and synthesis methods of nanocomposites

The interesting behavior of composites is typically attributed to the phenomenon called "nano-effect" i.e. the huge contact area due to the use of nano-sized fillers.

This leads to the formation of a very large interface area[25] between organic and inorganic phase, typically varying between 2 and about 50 nm, in which the interface material can represent up to 50% of the total volume of the material.

[25] **Interface area:** is the surface, or better to say, all the areas of separation between the matrix and the reinforcement in a composite.

This does not happen in the conventional composites where the interface constitutes a very small fraction (only the 1%) of the volume of all the material

This large amount of reinforcement surface area means that a relatively small amount of nanoscale reinforcement can have an observable effect on the macroscale properties of the composite.

Therefore, it is scientifically confirmed that the interface controls the extent of interaction between the filler and the polymer, determining the final properties of the composite.

Thus, to improve the properties of nanocomposites, it is essential to define a understanding and controlling process of its preparation.

As regards the production of polymeric nanocomposites, treated in this research activity, will be now described some of the techniques most widely used in literature, such as:

- ***Direct mixing:*** traditional technique for the realization of composite, it allows also to prepare nanocomposites. This technique requires the mixing of the phases, with a mechanical process, at the melting or softening temperature of the polymer.. The process is fast and simple and presents the advantage of not use solvents. However, for some polymers the introduction of a nanofiller can cause the increase of viscosity (making the process more difficult) or can lead to the degradation of the polymer [12].
- ***Polymerization in situ:*** this technique requires the dispersion of nanofillers in the precursor of the polimeric matrix, monomer[26], in order to allow subsequently the polymerization reaction. Fig.2.3 represents the various stages of the process.

[26] **Monomer:** in chemistry, this term defines a simple molecule having functional groups such that it is capable of combining recursively with other molecules (identical to itself or reactively complementary to itself) to form macromolecules. the term is also used to identify the repetitive structural unit which forms a polymer (more properly known as "repeat unit" of the polymer). The process of transformation of the monomer to polymer is called polymerization. When the monomers are used to produce copolymers, are called comonomer.

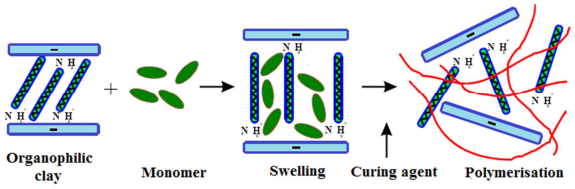

Fig.2.4: Polymerization in situ.

The viscosity of the monomers is considerably lower than that of the corresponding polymers and this condition certainly facilitates the dispersion of the fillers [13].

- ***Intercalation of the polymer in solution:*** is a two-stage process where in the first one, the mixing of the inorganic phase and the polymer occurs in the presence of a solvent, while in the latter the solvent is removed [14]. This technique is shown in Fig.2.5.

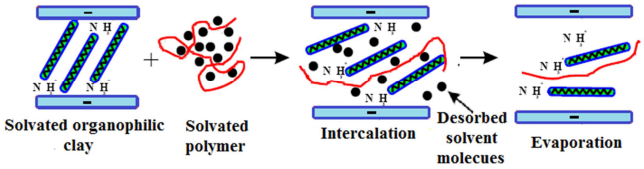

Fig.2.5: Intercalation of the polymer in solution

The limit of this method depends on the presence of the solvent, and therefore from the need to remove it.

- ***Direct Intercalation of the fused polymer:*** the filler, suitably modified, is mixed with the polymer to temperatures above the glass transition T_g[27] [14,15]. This process is shown schematically in Fig.2.6.

[27] **Glass transition Tg:** is the reversible transition in amorphous materials (or in amorphous regions within semicrystalline materials) from a hard and relatively brittle state into a molten or rubber-like state. This transition coincides with the activation of certain motions of the macromolecules that make up the material.. Below the Tg, polymer chains have difficulty moving and have locked positions and therefor it has a fragile elastic behavior.

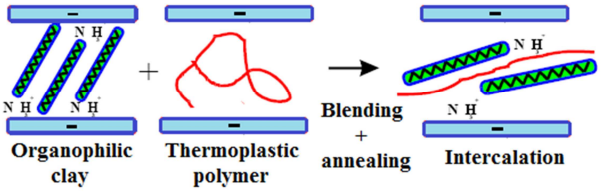

Fig.2.6: Direct Intercalation of the fused polymer

This method has a great potential for industrial exploitation, also because it has been obtained by extrusion of different thermoplastics, such as polyamides and polystyrene.

This manufacturing technology can be applied with all types of nanofillers available.

2.5 Percolation theory

In 1957, Broadbent[28] and Hammersley[29] presented a statistical theory, called *percolation theory*, useful to explain the behavior of disordered systems [16]. Since the publication of these early works, the percolation theory has been applied with excellent results in different fields such as chemical, physical, biological and others.

In summary, the original model, , is based on the idea of treating percolation as the passage of a fluid through a porous medium represented by a cubic lattice, as shown in Fig.2.7.

---

[28] **Broadbent:**Simon Ralph Broadbent was born in 1928: He studied engineering in Cambridge, mathematics at Magdalen College in Oxford (where he alsi wrote poetry) and started a PhD in statistic at Imperial College in London on “Some tests of departure from uniform dispersion”. During his PhD he got some support from the British Coal Utilisation Research Association to investigate statistical problems that could be related to coal production. In 1954 a symposium on Monte Carlo methods sponsored by the Atomic Energy research Establishment was held at the Rpyal Statistical Society in London.

[29] **Hammersley:** John Michael Hammersley (21 March 1920-2 May 2004) was a British mathematician best known for his foundational work in the theory of self-avoiding walks and percolation theory. He was born in Helensburgh in Dunbartonshire, and educated at Sedbergh School. He started reading mathematics at Emmanuel College, Cambridge but was called up to join the Royal Artillery in 1941. During his time in the army he worked on ballistics.He graduated in mathematics in 1948. He held a number of positions, both in and outside academia. His book Monte Carlo Methods with David Handscomb was published in 1964. He was an advocate of problem solving, and an opponent of abstraction in mathematics, taking part in the New math debate. He was a Reader at Oxford University from 1969, and elected Fellow of the Royal Society in 1976.

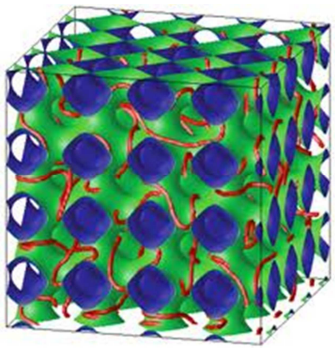

Fig.2.7: Percolation model: passage of a fluid through a porous medium represented by a cubic lattice.

The passage of fluid between the opposing faces of a generic cube, or of a sequence of cubes, is considered a random phenomenon.

Therefore, the model can be extended to all those problems where it is necessary to study the properties of global connection of a macroscopic system, whose connections are made at the microscopic level in a stochastic manner [17].

In general, percolation theory is a statistical theory which studies the formation of clusters and the existence of percolation phenomena in certain sites and links. It requires that at the base of the system there is the existence of a regular lattice. The cluster is the set of adjacent occupied sites within the lattice, while the percolation threshold is its probability of percolation in the system.

Different search algorithms are available to detect and study any percolative paths within the lattice.

Currently, percolation describes properties related to the connectivity of large numbers of objects which individually have some spatial extent, and for which their spatial relationships are relevant for specific applications.

A percolation problem that had received great attention in recent years concerns the electrical conductivity of nanocomposites.

In fact, percolation theory also answers the questions about the electrical conductivity of an incompletely connected network of conductive particles as well as occurs in such materials [19].

Just to give an idea, a simple electrical percolation problem can be represented by the random distribution of conductive particles (filler)

in an insulator matrix. If two particles are sufficiently neighbors (*tunneling distance*, that will be clarified in the following paragraphs) or in contact, a current could pass from one to the other. If the number of filler is high enough to reach a critical density, a continuous connected path through particles can be established. This path will conduct electricity.

In general, several factors, such as amount of filler, its nature and geometry, matrix type, technology process may influence the formation of the path and the resulting electrical conductivity [20].

2.6 Electrical Percolation Threshold (EPT) and conductivity in composites

The choice of carbon nanotubes, as conductive filler, in polymeric composites is adopted in many studies in the literature and scientifically justified since the substantial improvement in electrical conductivity composite, also for low concentration of nanotubes [20].

Furthermore, the increase in current carry capability doesn't affect the others characteristics of material, such as, for example, optical and mechanical properties, melting point etc.

The electrical conductivity of the nanocomposites essentially depends on the amount (typically expressed in volume or weight percentage) of filler added to the polymeric matrix.

For low filler content, the average distance between the conductive particles is large and don't allow the electrons flow from one particle to another. Therefore, the conductivity is limited and takes values typical of an insulating material which is the polymeric matrix.

Otherwise, in composite materials, containing conductive fillers, is observed an electrical conductivity increase when the concentration of this charges reaches a certain critical value, known as the *electrical percolation threshold* (EPT) at which filler particles form a percolating network through the composite.

Thus, an abrupt change occurs in the properties of composites near this threshold (see Fig.2.8), especially when there is a larger

difference between the properties of the different components of the composites [22].

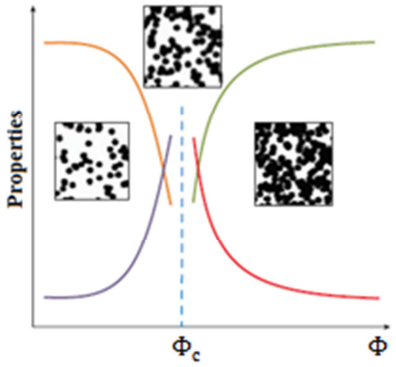

Fig.2. 8: Schematic of nonlinear changes in the properties (the four curves denote different property parameters) of composites near the percolation threshold ∅C (dashed blue line). The insets show the geometric phase transition of fillers (denoted by dark spots) in the composites' microstructure near percolation [22].

Generally, near percolation, these physical properties of composites can be described by the following explicit law:

$$Properties \propto |\Phi - \Phi_C|^{\pm e} \qquad 2.1$$

where *e* is a well-known critical exponent that is different for various properties, $\emptyset_C$ is the percolation threshold and $\emptyset$ is the instantaneous concentration of filler.

More specifically, as concerns the electrical conductivity, around this critical concentration it changes drastically of several orders of magnitude for small variations of the filler introduced, as shown in Fig. 2.9.

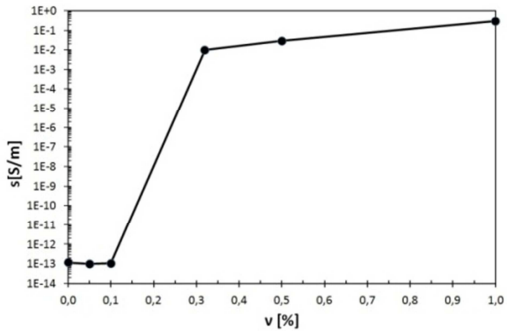

Fig.2. 9: Dc conductivity *vs.* filler concentration.

Achieved this threshold, the conductivity changes only slightly for further increase of filler.

In other terms, in percolation systems, there is a critical volume or weigth fraction below which the electrical properties are dominated by the insulating component and above which the conducting component dominates[23].

Such percolation systems are best analyzed using the two-exponent phenomenological percolation equation (TEPPE) that describe the electrical conductivity of composite in the regions below and above threshold:

$$\frac{(1-\Phi)(\sigma_i^{1/s}-\sigma_m^{t/s})}{\sigma_i^{1/s}-A\sigma_m^{1/s}}+\frac{\Phi(\sigma_c^{1/s}-\sigma_m^{t/s})}{\sigma_c^{1/t}-A\sigma_m^{1/t}}=0 \qquad 2.2$$

This equation gives a phenomenological relationship between σ_c , σ_i, and σ_m , which are the conductivities of the conducting and insulating component and the mixture of the two components, respectively [24]. Instead Φ_c is the percolation threshold, Φ is the volume fraction of CNT, $A=(1-\Phi)/\Phi_c$, *s* and *t* are exponents depending on the topological complexity of the obtained CNT structure. It is generally accepted that values of *t* in the range of 1.6-2.0 are representative of a three dimensional organization of the percolating structure.

The conducting volume fraction Φ ranges between 0 and 1 with Φ=0 characterizing the pure insulator substance ($\sigma_m=\sigma_i$) and Φ=1 the pure conductor substance ($\sigma_m=\sigma_c$) [25].

For $s=t=1$ the equation yields the two limits:

$$|\sigma_c| \to \infty: \qquad \sigma_m = \sigma_i \frac{\Phi_c{}^s}{(\Phi_c-\Phi)^s} \qquad \forall\ \Phi < \Phi_c \qquad 2.3$$

$$|\sigma_i| \to 0: \qquad \sigma_m = \sigma_c \frac{(\Phi-\Phi_c)^t}{(1-\Phi_c)^t} \qquad \forall\ \Phi > \Phi_c \qquad 2.4$$

In the case that $\Phi_c << 1$ and $\Phi_c<\Phi$ the equation 2.4 can be rewritten in the form:

$$\sigma_m = \sigma_c(\Phi - \Phi_c)^t \qquad \forall\ \Phi > \Phi_c \qquad 2.5$$

which is an equation known as *percolation law*, universally used to describe the composite conductivity for which the electrical percolation threshold is reached or exceeded.

The distribution of fillers in a matrix plays a key role in determining EPT, which is influenced mainly by the geometric parameters, such as particle size, shape, and orientation.

CNT-based composites usually exhibit very low percolation thresholds (concentration of the nanotubes from 0.005% to few percent values) due to their high *aspect ratio* (ratio between lenght and diameter of the nanotube). These low typical values of the percolation threshold are mainly due to the quality of the dispersion of the nanotubes, i.e. their spatial distribution in the matrix.

Furthermore, it should be noted that Van Der Waals forces between the carbon nanotubes are generally stronger than those between polymers.These interactions, in addition to their size, determine a considerable phenomenon of aggregation of the tubes that typically reduces their aspect ratio and the number of separate bundles within the composite, increasing, therefore, the percolation threshold.

This means that dispersion of the nanotubes is crucial in determining the contribution to the final conductivity of composite [26].

2.7 Tunneling effect

In general, electrons in a polymer cannot transfer from one electrode to another through the insulator due to the existence of an energy barrier. Due to the unavoidable layer of insulating polymeric materials wrapping around the CNTs and short distance between them, the tunneling effect has been proposed to be the main mechanism responsible of governing the electrical conduction in such polymeric nanocomposites. In fact, CNTs-based polymer exhibit conductive behavior, which can be explained only as the tunneling of electrons one by one from the first CNT electrode to the next-nearest CNT electrode, forming a CNT/polymer pathway according to the percolation theory [27].

This means that, when a voltage is applied, the energy barrier shape changes and there is a driving force that moves electrons across the barrier by tunneling. This results in a overlapping of the electron wavefunctions extending from the two surfaces and then in a low current when the distance among neighboring particles is sufficiently small, as shown in Fig.2.10.

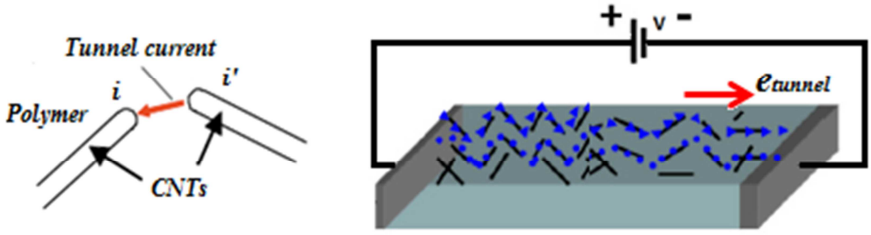

Fig.2.10: Schematic diagram illustrating pathways of electron tunneling through a nanocomposite.

Therefore, for this assumption, the conductivity of a nanocomposite should follow that of CNTs. Really, the resistivity of a nanocomposite isn't governed by the interconnected CNTs, but the polymer between neighboring CNTs because tunneling resistance plays a dominant role in the electrical conductivity of carbon nanotube–based composites [28].

This approach is consistent with the significant reduction of the composite resistivity with the addition of CNTs

There are many pathways for the electrons passing through two opposite electrodes placed in the composite. Therefore, the total current passing through the bulk nanocomposites is to add up the tunneling currents in each of the pathways.

An analytical expression for this tunneling current has been formulated by Simmons referring to the electric tunnel effect between similar electrodes separated by a thin insulating film [29].

If the thickness of the insulating layer, in the contact area of the nanotubes, is assumed uniform and the variation of the height barrier along the thickness negligible, the formula for a rectangular potential barrier can be employed.

When two metallic electrodes are separated by an insulating film, the equilibrium conditions require that the top of the energy gap of the insulator be positioned above the Fermi level of the electrodes, as shown in Fig. 2.11.

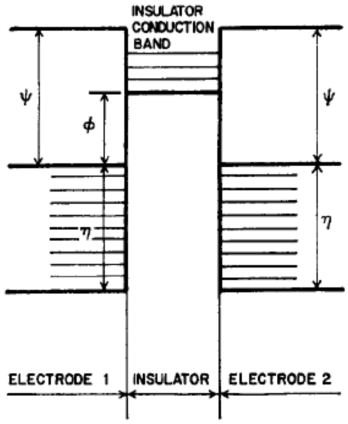

Fig.2.11: Rectangular potential barrier in insulating film between metal electrodes for V=O [29];

Thus, the action of the insulating film is to introduce a potential barrier between the electrodes which impedes the flow of electrons between the electrodes. The electronic current can flow through the insulating region between the two electrodes if:

- the electrons in the electrodes have enough thermal energy to surmount the potential barrier and flow in the conduction band;

- the barrier is thin enough to permit its penetration by the electric tunnel effect.

Conditions that can be favored by applying a suitable voltage. The current density penetrating the insulating film can be expressed as:

$$J = 6.2 * 10^{10}(\Delta t)^{-2}\left[\varphi e^{-\left(1.025\Delta t\varphi^2\right)} - (\varphi + U)e^{-\left(1.025\Delta t(\varphi+U)^{0.5}\right)}\right] \quad 2.6$$

where:

$$\varphi = \varphi_0 - \frac{U}{2t}(t_1 + t_2) - \frac{5.75}{K\Delta t} ln \frac{t_2(t - t_1)}{t_1(t - t_2)} \quad 2.7$$

t is the thickness of insulating film (in Å) and $\Delta t = (t_2 - t_1)$ is the difference of the limits of barrier at Fermi level with:

$$t_1 = 6/K\varphi_0 \quad 2.8$$

$$t_2 = t[1 - 46/(3\varphi_0 Kt + 20 - 2UKt)] + 6/K\varphi_0 \quad 2.9$$

The symbol φ_0 denotes the rectangular potential barrier, k is the dielectric constant of insulating material while U is the voltage across the film and can be evaluated by:

$$U = e/C = e * t/A_C K\varepsilon_0 \quad 2.10$$

where e is the electron charge, C represents the capacitance, and ε_0 is the permittivity of vacuum.

The tunneling resistivity (in Ωcm^2) of the insulating film can be given by:

$$\rho_{tunnel} = U/J \quad 2.11$$

and therefore the tunneling resistance obtained by:

$$R_{tunnel} = \rho_{tunnel}/A_C \quad 2.12$$

As shown in Fig.2.12, the thickness of insulating layer between neighbors CNTs plays a significant role in the tunneling resistance, which increases very rapidly with increasing layer thickness.

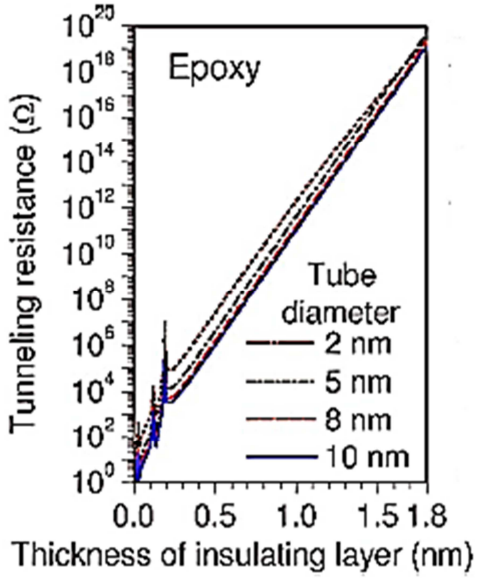

Fig.2.12: Tunneling resistance as a function of the thickness of an insulating layer and the CNT diameter [28].

When the thickness is 1.0 nm, the tunneling resistances are in the order of 100 $G\Omega$, which is several orders of magnitude larger than the contact resistance evaluated between CNTs without an insulating layer.

Instead, the CNT diameter has a negligible effect on the tunneling resistance even if with the increase of the diameter of the tube, slightly decreases the resistance of tunneling.

2.8 Industrial applications of nanocomposites

Nanosciences and nanotechnologies are new scientific and technologic approaches aim to check the structure and behavior of matter at the atomic and molecular level.

Nanocomposites offer to industry a number of advantages mainly related to their weight and singular performance. It is not obviously possible to bring together the individual benefits in a single

composite. It is therefore necessary to find a good balance among the most important properties and the possible side effects, such as, for example a more complex rheological behavior and a greater difficulty in processing.

The application fields of nanocomposites can be several, as shown in Fig.2.13, because the properties that can be increased are many and varied.

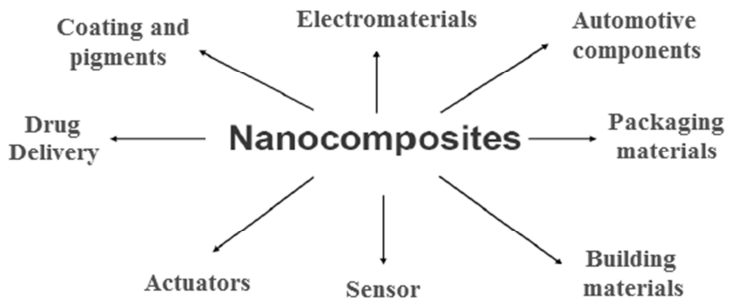

Fig.2.13: Some nanocomposites applications.

Among this applications there are:

- ***Nanocomposite solar cells****:* polymer-based solar cells can be used to make cheap large flexible panels. The only downside is substantially low efficiency compared to commercial solar cells. Several efforts are being taken to improve the efficiency of the cells. In general, it was observed that a higher density of nanoparticles is advantageous
- ***Nanocomposite membrane for gas separation and gas permeability:*** various inorganic filler have dispersed in polymer matrices to improve pure polymeric membrane properties and form mixed-matrix membranes (MMMs). The presence of minimum amount of nanoparticles, allows significant increasing in permeability of membrane.
- ***Nanocomposite with gas barrier performance****:* by addition alumina silicate layers to polymer matrix can be obtained a nanocomposite with gas barrier function.
- ***Aerospace application:*** composite materials are particularly attractive to aviation and aerospace

applications because of their exceptional strength and stiffness-to-density ratios and superior physical properties. Initially, composite materials were used only in secondary structure, but as knowledge and development of the materials has improved, their use in primary structure such as wings and fuselages has increased. The use of composite materials in commercial transport aircraft is attractive because reduced airframe weight enables better fuel economy and therefore lowers operating costs.

References

[1] William D. Callister, Material Science and Engineering: An Introduction, 5ª ed., John Wiley & Sons Inc, 1999

[2] A. Lagashetty, A. Venkataraman "Polimer Nanocomposites", Resonance, Volume 10, Number 7, 49-57, July 2005

[3] Sanjay K. Mazumdar, "Composites manufacturing: materials, product, and process engineering", CRC Press, 2002

[4] TC229 Nanotechnologies, www.iso.org, 2005

[5] P.M. Ajayan; L.S. Schadler; P.V. Braun, "Nanocomposite science and technology", Wiley, 2003.

[6] T.J. Pinnavaia, G.W. Beall, "Polymer-Clay Nanocomposites" Wiley, New York, 2001.

[7] S.S. Ray, M. Bousmina, "Polymer Nanocomposites and Their Applications",American Scientific, Stevenson Ranch, CA, 2006.

[8] H. Köpnick, M.Schmidt, "*Polyesters*", Ullmann's Encyclopedia of Industrial Chemistry, 2000.

[9] L.Guadagno, B. De Vivo, A. Di Bartolomeo, P. Lamberti, A. Sorrentino, V. Tucci, L. Vertuccio, V. Vittoria, "Effect of functionalization on the thermo-mechanical and electrical behavior of multi-wall carbon nanotube/epoxy composites" ,Carbon. Vol. 49,pp.1919-1930,2011.

[10]L. Guadagno, C. Naddeo, V. Vittoria, A. Sorrentino, L.Vertuccio, M. Raimondo, V. Tucci , B. De Vivo, P. Lamberti, G. Iannuzzo,E. Calvi, S. Russo, "Cure behavior and physical properties of epoxy resin-filled with multiwalled Carbon nanotubes", Journal Of

Nanoscience And Nanotechnology, Vol. 10 (4), pp.2686-2693,2010.
[11] W. Krenkel, “Ceramic Matrix Composites”. Wiley-VCH, 2008
[12] R. J. Young, P. A. Lovell, “Introduction to Polymers”, 2nd edition, Chapman and Hall, 1991.
[13] G. Odian, “Principles of Polymerization”, 3rd, Wiley, 1991.
[14] J.M.G. Cowie "Polymers:Chemistry and Physics of Modern Materials”, Chapman and Hall, 2d.1991
[15]S. L. Rosen, “Fundamental Principles of Polymeric Materials”, 2nd ed., Wiley,1993.
[16]S. R. Broadbent, J. M. Hammersley, “Percolation processes. I. Crystals and Mazes”, Proceedings of the Cambridge Philosophical Society, vol. 53, no. 3, pp. 629-641, 1957.
[17]M.Sahimi, “Applications of Percolation Theory”, Taylor&Francis, 1994.
[18]D.Stauffer, A. Aharony, “Introduction to Percolation Theory”, taylor & Francis, 2010.
[19]A.J.Hunt, “Percolation Theory for flow in porous media”, Springer, 2005.
[20] B. De Vivo, A . Di Bartolomeo, L. Guadagno, P. Lamberti, M.L. Raimondo, V. Tucci, V.Vittoria, “Nanofillers in epoxy resins for multifunctional materials: from electrical to barrier properties”. World Journal Of Engineering. Pag.975-976, 2009.
[21]J. Sandler, M.S.P. Shaffer, T. Prasse, W. Bauhofer, K. Schulte, A.H. Windle, “Development of a dispersion process for carbon nanotubes in an epoxy matrix and the resulting electrical properties”. Elsevier Science Ltd, Vol.40,Issue 21, pp 5967-5971, 1999.
[22] C.W. Nan, Y. Shen, Jing Ma, “Physical Properties of Composites Near Percolation”, Annu. Rev. Mater. Res. 40, pp.131–151, 2010.
[23] D. S. McLachlan, G. Sauti, “The AC and DC Conductivity of Nanocomposites”, Journal of Nanomaterials,2007.
[24] D. S. McLachlan, W. D. Heiss, C. Chiteme, and Junjie Wu, “Analytic scaling functions applicable to dispersion measurements in percolative metal-insulator systems”, Physical Review B, Vol. 58, N20, 1998.

[25] D. S. McLachlan, G. Sauti, K. Cai, “AC and Dc conductivity-based microstructural characterization”, International Journal of Refractory Metals & Hard Materials, pp-437-445, 2001.

[26]D. K. James, J. M. Tour, “Electrical Measurements in Molecular Electronics,” *Chem. Mater.*, *1*6, pp.4423-4435,2004.

[27] C Gau, Cheng-Yung Kuo and H S Ko, “Electron tunneling in carbon nanotube”, Nanotechnology 20, 2009.

[28] Chunyu Li, E. T. Thostenson, Tsu-Wei Chou, “Dominant role of tunneling resistance in the electrical conductivity of carbon nanotube–based composites”, Applied Physics Letters 91, 2007.

[29] J.Simmons, “Generalized Formula for the Electric Tunnel Effect between Similar Electrodes Separated by a Thin Insulating Film”, Journal Of Applied Physics, Vol.34, 1963

Chapter 3

Electromagnetic properties of CNT-based composites

Although in recent years considerable efforts have been dedicated to the production of nanocomposites, many aspects concerning the underlying physical mechanism responsible of their properties still remain to be clarified. To reach this goal interdisciplinary research activities are required.
In this perspective, the electromagnetic characterization of nanocomposites is of considerable scientific importance helping to understand, adapt and optimize their properties.. For this purpose in this thesis simple CNT-epoxy systems or multi-phase composites (epoxy/CNT/clay) have been considered in a wide experimental characterization activity. The aim of this characterization is to highlight possible correlations between morphological characteristics of the different fillers and electrical properties of the nanocomposites.

3.1 Motivation and objectives

Research activities in CNT-based composites have made enormous progress towards the production of next-generation advanced structural materials characterized by thermal, optical, and electrical advantages.

However, some questions about these composites concerning for example, the filler dispersion, its alignment, interface with matrix remain only partially clarified.

With reference to the interesting properties observed in the nanocomposites and to issues still open, the experimental research aims to investigate to electrical properties, responses and possible

connections between performance and morphology, as well as variations due to different dispersed phase concentrations.

To highlight possible correlations between performance and morphology, research activity has focused on two classes of nanocomposites, kindly provided by the group of Chemistry for Technology (proff. V. Vittoria and L. Guadagno) of the Dept. of Industrial Eng. Of the University of Salerno. Both composites contain the same conductive filler (MWCNTs) but they differ because one of them presents also a nanoclay (Hydrotalcite[30]), at two different concentrations (0.1% and 1% in weight).

The latter was introduced in order to evaluate the effect of morphology on the dispersion of carbon nanotubes in the matrix and the possible influences on the final performance of the composite.

The systems were tested at various filler concentrations, which were nearby the percolation threshold to highlight possible connections between the percolated structure and dielectric performance.

In any case the reference for the comparison of the performance is always the pure polymeric matrix while the comparison between the different systems is carried out at the same conductive filler content.

The electrical characterization has involved DC and AC conductivity measurements of the systems at different temperature.

The activity was conducted on innovative composite materials since of multi-phase type (polymer/CNT/Clay) and therefore a novelty in literature.

A preliminary investigation seems to be appropriate in order to assure the basic influence that the nanoclay induces in the material especially in terms of the electrical conductivity. To this aim, DC measurement are performed and presented in the next part.

The aim is to identify the combination of factors that maximizes the performance of the composite and to pursue an "ad hoc design".

This can give the possibility of having a tailored material as well as build systems with controlled and reproducible properties.

---

[30] **Hydrotalcite:** is a layered double hydroxide of general formula $Mg_6Al_2(CO_3)(OH)_{16}\cdot 4(H_2O)$ whose name is derived from its resemblance with talc and its high water content. It is an anionic clay found in nature. It has also a variety of pharmaceutical applications.

3.2 Preparation and characteristics of the composites

The composites are manufactured by using as base epoxy resin DiGlycidil-Ether Bisphenol-A (DGEBA), with 4,40-diaminodiphenyl sulfone (DDS), as hardener agent.

The MWCNTs (3100 Grade), obtained from Nanocyl S.A, are characterized by a diameter of about 10 nm and an average length variable in the range of 0.1÷1 μm . A SEM image is shown in Fig. 3.1

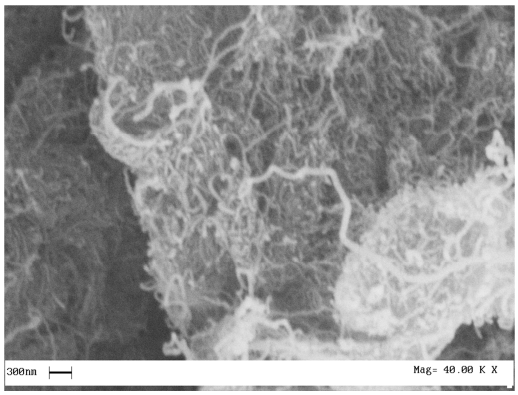

Fig.3.1:SEM image of the adopted MWCNTs

Epoxy and DDS were mixed at 120 °C and the MWCNTs togheter with Hydrotalcite (see Fig.3.2), for the second type of composite, were added and incorporated into the matrix by using a ultrasonication[31] for 20 min.

Such an incorporation method has been chosen among other different techniques since it leads to the composites characterized by the best mechanical and electrical properties [1].

[31] **Ultrasonication:** is the act of applying sound (usually ultrasound) energy to agitate particles in a sample, for various purposes. In the laboratory, it is usually applied using an ultrasonic bath or an ultrasonic probe, colloquially known as a sonicator. Sonication can be used to speed dissolution, by breaking intermolecular interactions. It may also be used to provide the energy for certain chemical reactions to proceed and commonly used in nanotechnology for evenly dispersing nanoparticles in liquids.

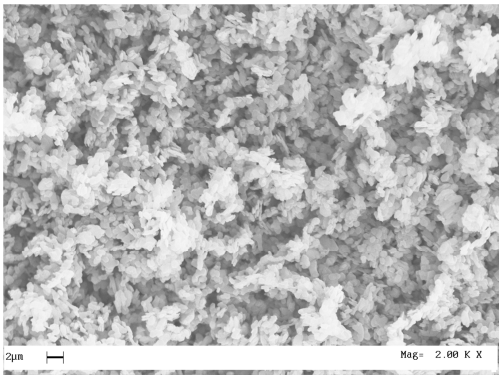

Fig.3.2: SEM image of Hydrotalcite

At the end of the production process, the samples appear in the form shown in Fig. 3.3

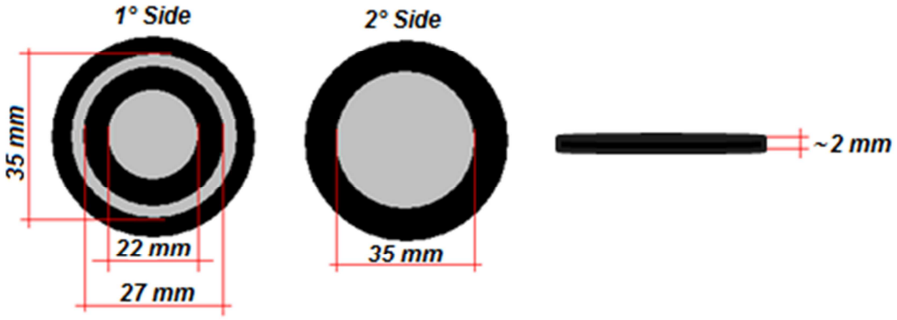

Fig.3 3: Sample geometry

The same figure shows also the metallization (in accordance with CEI Standard 15-23[32]) on the samples made with silver paint (Silver Coated Copper Compound Screening - RS 247-4251, surface resistivity 0.7 Ω-square and thickness of about 50µm) and the possible guard ring for the characterization of samples with low resistivity.

The size and characteristics of the individual samples are illustrated in the following tables.

[32] **CEI Standard 15-23:** defines methods of the test for volume resistivity and surface resistivity of solid electrical insulating materials.

A first family of samples, classified as “C1-Epoxy-80DDS-NST” is made with epoxy resin and carbon nanotubes at various concentrations, as reported in Table 3.1.

Table 3.1: C1-Epoxy-80DDS-NST

Samples	% CNT	Type of CNT	% Clay	Type of Clay	Total charge	Thickness[mm]
Epoxy-80DDS-NST	0	MWCNT	//	//	0	1.8
Epoxy-80DDS-0.05% CNT- NST	0.05	MWCNT	//	//	0.05	2.4
Epoxy-80DDS-0.1% CNT- NST	0.1	MWCNT	//	//	0.1	2.38
Epoxy-80DDS-0.3% CNT- NST	0.3	MWCNT	//	//	0.3	2.18
Epoxy-80DDS-0.5% CNT- NST	0.5	MWCNT	//	//	0.5	2.28
Epoxy-80DDS-1% CNT- NST	1	MWCNT	//	//	1	2.38

Instead, as shown in Table 3.2, a second family of samples, called “C2-80DDS-01HT” always made with epoxy resin and MWCNTs at various concentrations contains also Hydrotalcite in concentration of 0.1% in weight.

.

Table 3.2:C2-Epoxy-80DDS-01HT

Samples	% CNT	Type of CNT	% Clay	Type of Clay	Total charge	Thickness[mm]
Epoxy-80DDS-0.1HT	0	MWCNT	0.1	Hydrotalcite	0.1	1.95
Epoxy-80DDS-0.05% CNT- 0.1HT	0.05	MWCNT	0.1	Hydrotalcite	0.15	1.88
Epoxy-80DDS-0.1% CNT- 0.1HT	0.1	MWCNT	0.1	Hydrotalcite	0.2	2.32
Epoxy-80DDS-0.3% CNT- 0.1HT	0.3	MWCNT	0.1	Hydrotalcite	0.4	2.68
Epoxy-80DDS-0.5% CNT- 0.1HT	0.5	MWCNT	0.1	Hydrotalcite	0.6	2.36
Epoxy-80DDS-1% CNT- 0.1HT	1	MWCNT	0.1	Hydrotalcite	1.1	2.24

Finally, the features of a third family of samples, “C3-80DDS-1HT”, equal to the second but with a slightly higher concentration of nanoclay (1 wt%), are summarized in Table 3.3. The further increase of the clay is aimed at defining an optimal concentration of the clay.

Table 3.3:C3-Epoxy-80DDS-1HT

Samples	% CNT	Type of CNT	% Clay	Type of Clay	Total charge	Thickness[mm]
Epoxy-80DDS-0.1HT	0	MWCNT	1	Hydrotalcite	1	1.95
Epoxy-80DDS-0.05% CNT- 1HT	0.05	MWCNT	1	Hydrotalcite	1.05	1.88
Epoxy-80DDS-0.1% CNT- 1HT	0.1	MWCNT	1	Hydrotalcite	1.1	2.32
Epoxy-80DDS-0.3% CNT- 1HT	0.3	MWCNT	1	Hydrotalcite	1.3	2.68
Epoxy-80DDS-0.5% CNT- 1HT	0.5	MWCNT	1	Hydrotalcite	1.5	2.36
Epoxy-80DDS-1% CNT- 1HT	1	MWCNT	1	Hydrotalcite	2	2.24

3.3 Percolation and electrical conductivity

The performance of a CNT-based composite is sensitive to the dispersion and arrangement of filler within the polymer matrix, therefore it is important to control the production process of the polymer/particle mixtures but also the resulting morphology, topic not still sufficiently clarified. Literature data confirm that morphology is important with respect the electrical DC properties [1].

The introduction of an additional filler together with carbon nanotubes can be an alternative and a novelty, with the respect to the classical nanocomposites, for changing their properties.

Therefore, nanoclay such as Hydrotalcite (henceforth HT), are used in the preparation of our polymer-based composites hoping to improve the dispersion of MWCNTs and hence the final conductivity of the nanocomposites.

For this purpose, the two different concentrations of clay (0.1 wt% and 1wt%) must allow to detect any benefits or disadvantages deriving from the greater or lesser percent loading of this filler.

Such a response can be provided through measurements of the dc volume conductivity that also allow to determine if the analyzed sample presents or less percolation phenomena.

The measurement system, remotely controlled by the software LABVIEW®, is composed of a pico-ammeter Keithley 6514 (min current 100aA), multimeter HP 34401A and a suitable shielded cell with temperature control.

For sensitivity purposes the applied electric field has been 3 kV/m for samples at low CNT concentration (0.05 wt% and 0.1 wt%), whereas in order to avoid Joule heating of samples it has been set to 1.5 kV/m for the ones above this concentrations, obviously taking costant the electrode areas. Instead, an electric field of 5 MV/m has been applied for the samples without CNT regardless of the presence of clay.The analysis of the conductivity as a function of concentration υ of MWCNTs allows to evaluate the behavior in terms of percolation of the different nanocomposite systems.

Some of these obtained experimental results are presented and discussed. For example, the Fig.3.4 shows the conductivity for the system C1 (Epoxy 80DDS-NST) as function of concentration υ of MWCNTs, at room temperature (30 °C).

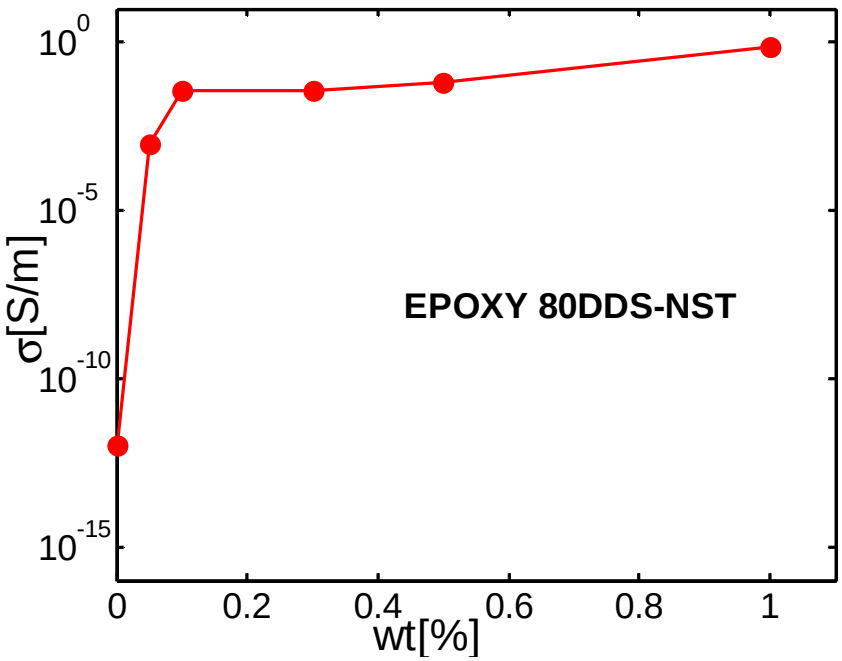

Fig.3 4: Conductivity for the system C1 at the room temperature (30°C)

DC conductivity vs the filler concentration shows the typical percolation curve of the composite.

In fact , in this range of CNT content (0.05 – 1 wt%), according to the percolation theory, a threshold appears, and a jump of more than 5-6 order of magnitude in the dc electric conductivity is observed.

Instead, the Fig.3.5 shows the DC conductivity for the system C2 (Epoxy 80DDS-01HT), always at room temperature (30 °C).

Also in this case, for all CNT concentrations percolative phenomena are present . In fact, in the absence of percolation the material behaves as an "insulator" and an electric conductivity very similar in the value to that of the unfilled matrix ($\sigma \sim 10^{-12}$ S/m) is obtained.

On the contrary, beyond the percolation threshold, a conductive composite is obtained and a DC conductivity of about 1 S/m is expected.

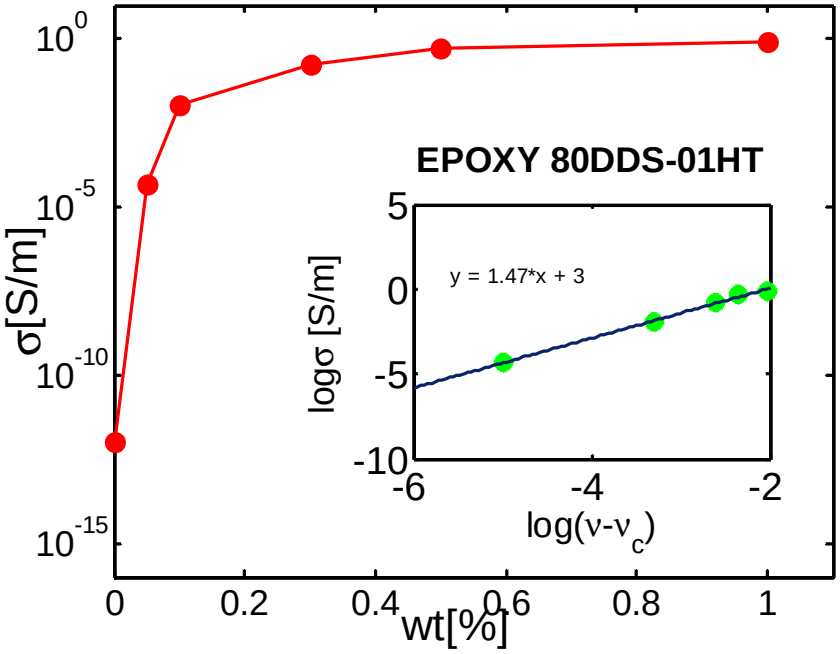

Fig.3. 5: Conductivity for the system C2 at the room temperature (30°C)

In the inset of the Fig.3.5, the fitting curve is reported in order to obtain the classical parameters of the percolation law.

In fact, the DC measurement leads to calculate the characteristic parameters of the percolation law, such as the critical exponent *t* or the

percolation threshold v_c, by adopting the following equation of conductivit:

$$\sigma = \sigma_0(\nu\text{-}\nu_c)^t \qquad 3.1$$

This expression rewritten in logarithmic terms provides a linear equation:

$$log(\sigma) = log(\sigma_0) + t \cdot log(\nu\text{-}\nu_c) \qquad 3.2$$

useful to extract the desired information by means interpolation technique. The equation (3.1) is valid for the DC data obtained for specimen after the percolation.

Moreover, the DC measuraments have been permormed for other values of temperature (30, 50, 70, 90, 110 ° C) leading to obtained the classical parameters of the percolation law, reported in Table 3.4.

Table 3. 4: Characteristics parameters for the system C2 Epoxy 80DDS-01HT

T[°C]	C2 - Epoxy 80DDS-01HT			
	T	**Log(σo)**	**υ_c[%]**	**R^2**
30	1,4697	3,0025	0.049	0,9958
50	1,4799	3,0571	0.049	0,9966
70	1,4815	3,0646	0.049	0,9967
90	1,4815	3,0663	0.049	0,9968
110	1,4802	3,0623	0.049	0,9973

By looking at this Table it is possible to see that the estimated percolation threshold is 0.049 wt %. The high value of R^2, close to 1, confirms the goodness of the interpolation.

The measurements of the dc volume conductivity for the system C3 (Epoxy 80DDS-1HT), performed at room temperature (T=30°C) and at various MWCNT loadings, are reported in Fig.3.6.

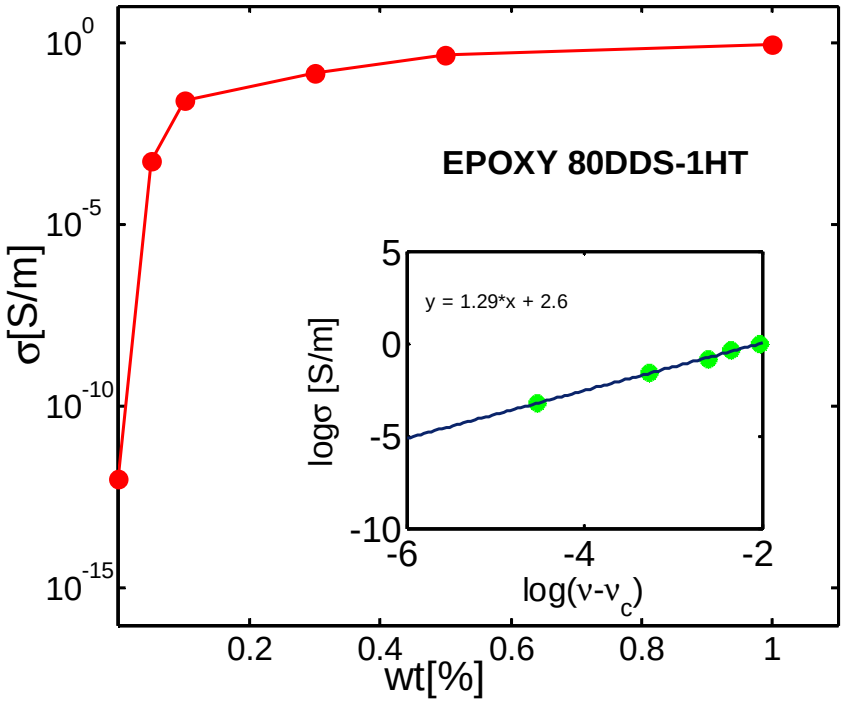

Fig.3.6: Conductivity for the system C3 at the room temperature (30°C)

As expected, already the sample at υ=0.05 wt % assume a very high dc conductivity with respect to the unfilled material, i.e. $\sigma=5.61\cdot10^{-4}$ S/m and $\sigma \sim 10^{-12}$ S/m respectively.

It is possible to observe that this is a concentration above the percolation threshold and therefore the composite will assume an ohmic behavior. The characteristic parameters of the percolation law can be obtained by inspecting the fitting curve reported in the inset of the same figure. Also in this case all the measurement results, relative to the other temperatures (30, 50, 70, 90, 110 ° C) are shown, in terms of characteristic parameters, in Table 3.5 rather than graphically.

The estimated percolation threshold is only 0.047 wt%. The results for the exponent t, indicative of the topological complexity of the obtained CNT-based structure, are in the nearby of the theoretical prediction. Values in the range of 1.6-2 are representative of a 3D structural organization while values of t in the range of 1.1-1.3 are typical of two-dimensional systems [2],[3].

Table 3.5: Characteristics parameters for the system C3 Epoxy 80DDS-1HT

T[°C]	C3 - Epoxy 80DDS-1HT			
	t	**Log(σo)**	**υ_c[%]**	**R^2**
30	1,2904	2,6005	0.047	0,9971
50	1,2946	2,6317	0.047	0,9978
70	1,3025	2,6804	0.047	0,9984
90	1,3008	2,6756	0.047	0,9982
110	1,3014	2,6853	0.047	0,9983

With reference to this parameter it is important to note that the increase of the clay content (HT) from 0.1 wt% to 1 wt% causes a decrease of the exponent t, i.e. 1.469 and 1.290 respectively. This means that nanoclay favors a bi-dimensional disposition, somehow forcing the nanotube in its orientation.

Finally, in a single graph, as shown in Fig 3.7, the curves of the conductivity for the three systems are compared.

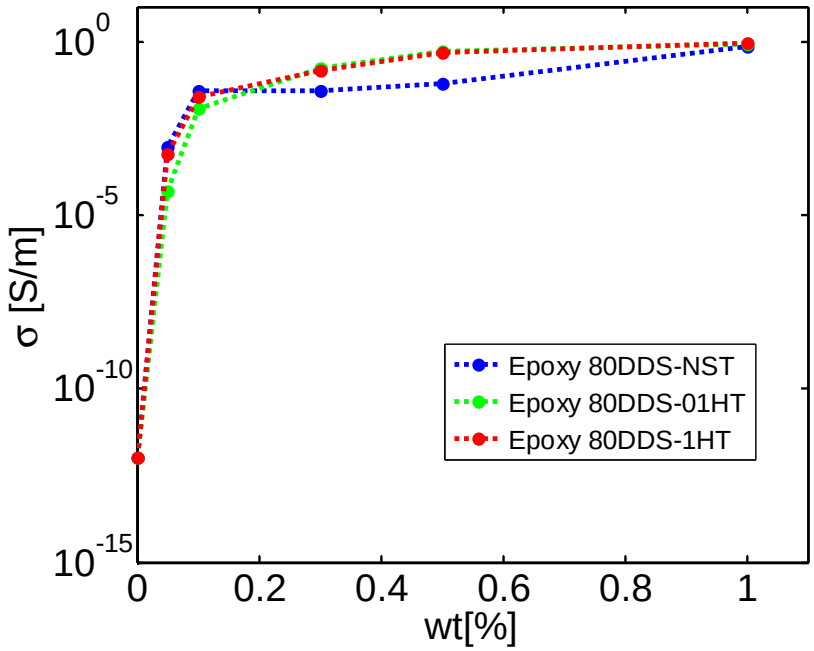

Fig.3.7: Comparison of the electrical performance

Analyzing this plot some conclusive considerations can be drawn. This results leads to confirm that the introduction of CNT induces a significant enhancement to the conductive properties of the nanocomposites.

The different systems exhibit an appreciable conductivity ($> 10^{-2}$S/m) already for low values of the concentration of MWCNTs ($\upsilon \leq 0.1\%$) showing a very low percolation threshold.

These so minimum concentrations to achieve the percolation threshold are certainly due to the use of epoxy-based resin in which carbon nanotubes can be easily dispersed with the sonication technique.

In fact, it is widely recognized that the dispersion state of CNTs has a significant influence on the electrical resistivity and percolation threshold of CNT-filled polymers.

Always as regards the percolation threshold, the investigation of the dc conductivity of two supplementary specimens (see Table 3.6 for the details), puts in evidence a remarkable difference between the two analyzed composites, i.e. with or without clay.

Table 3.6: Supplementary samples for inspection around the percolation threshold

Samples	% CNT	Type of CNT	% Clay	Type of Clay	σ (S/m)
Epoxy-80DDS-NST	0.025	MWCNT	0	Hydrotalcite	$9.30 \cdot 10^{-4}$
Epoxy-80DDS-1HT	0.025	MWCNT	1	Hydrotalcite	$5.14 \cdot 10^{-12}$

The corresponding values of the conductivity assure that υ=0.025 wt% of CNT content is a concentration after percolation, only for the composite without clay, i.e. 80DDS-NST (see Fig.3.8).

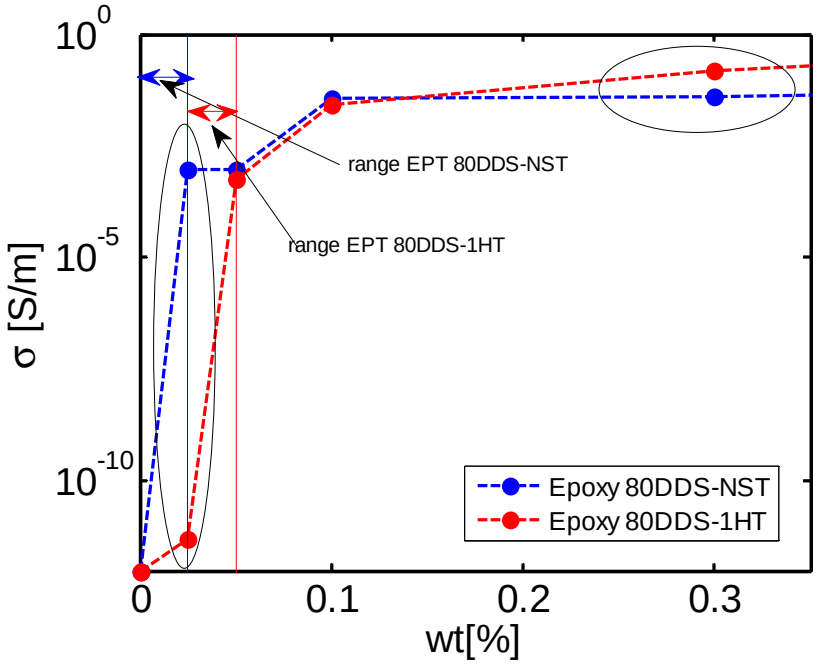

Fig.3.8: Comparison between EPT

This means that the presence of nanoclay induces a sensible increment to the percolation threshold. The Fig. 3.9 can provide a possible justification.

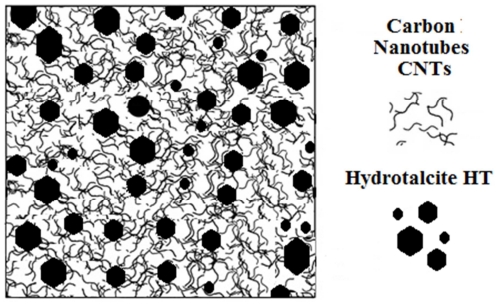

Fig.3. 9: Illustration of the influence of HT on the percolation threshold of the composite

The presence of Hydrotalcite, and therefore of clay, may hinder the formation of continuous paths useful for the electrical percolation

which is thus achievable only with a higher concentration of conductive filler (CNTs).

Another observable peculiarity is that, for low concentrations of CNT the conductivity of composites with clay (HT) is lower than the composite without clay whereas it become higher with the increase in the CNT concentration (see Fig.3.7 and Fig.3.8). In particular the conductivity of the composite C2 and C3 overcomes the C1 family for CNT content higher than $\upsilon = 0.2\%$ (see Fig.3.7), value at which the blue line intersect the red and green ones.

The Fig.3.9, used to justify the increase in the percolation threshold, could provide also in this case an acceptable motivation.

Incorporation of such nanoclay into CNT-filled polymers can reduce the space available for CNTs to form conductive networks and thus could increase the conductivity, since CNTs cannot diffuse into the fillers which are solid particles. This means that in the percolative paths the distances between the CNTs can be significantly reduced and since the tunneling strongly depends on this distance follows an increase in the conductivity.

The role of clay was to assist dispersion of the carbon nanotubes and thus result in better electrical proprieties.

Therefore, the production of polymer composites containing a low quantity of nanoclay can be an alternative to polymer blends for changing the properties of polymeric materials.

3.4 Optimization of the electrical conductivity

Multi-phase composites (polymer/CNT/clay) may contain different amounts of HT or CNT and exhibit different performance based on these values.

Therefore, we have tried to improve the properties of the composite.

In particular, the objective is to find the right combination of these parameters to achievethe enhancement of the electrical conductivity of such multi-phase systems.

The growing complexity of engineering systems has stimulated a deep interest in design methods able to ensure that the system

performance might vary in a predictable range, primarily in presence of variations of either the constituent physical parameters or the operating conditions [4].

Therefore, a theoretical approach able to predict in some way the real performance of the samples is fundamental to ensure that production meets the complex demands of required performances.

To use this approach in designing and analyzing an experiment, it is necessary to have, in advance, a clear and precise idea of exactly what is to be observed, how the data are to be collected, and at least a qualitative understanding of how the data are to be analyzed [5].

A guideline for a possible procedure is shown in Fig.3.10.

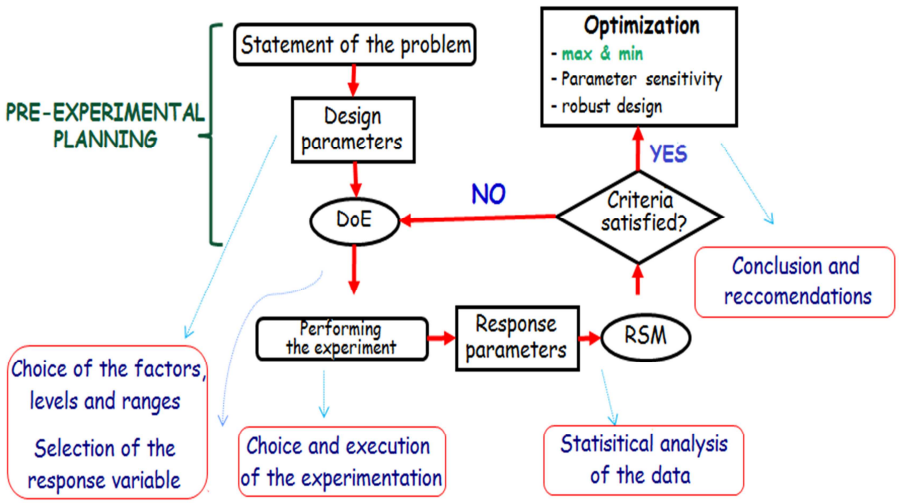

Fig.3.10: Guideline for designing an experiment

A brief discussion of of some key points adapted to the purposes of the research activity is presented.

3.5 Approximation of the performance function

The use of interpolation models for analyzing the phenomena that occur in a given system regarded as a "*black box*" is very common in systems of engineering interest.

In fact, if the performance function is not known in closed form but through the points obtained, for example, by means of experimental results or circuital simulations, it is possible to use of a suitable interpolation and operate on it [6].

From the experimental data an analytical model that correlates the output variable to the input ones, by means of appropriate interpolation techniques can be obtained.

Thus the behavior of the under test system can be represented in a synthetic manner and the output values can be evaluated also for a generic inputs.

On the obtained model, all necessary tests can be performed. In particular it is possible to apply optimization techniques to find the combination of inputs for which the performance function meets one or more requirements.

In this research, the performance function is represented by the DC conductivity "σ". It is a property that must be maximized, (for example as required in shielding applications) in order to have a conductive polymer and on which it is of interest to evaluate the effects of the design parameters.

In the present case, the parameters are the conductive filler concentration (f1%), the clay content (f2%) and the temperature (T°).

It is worth noting that f1% and f2% are fixed in the production phase while T° is taken as operating temperature controlled by means of a special room.

Analytically it is possible to summarize this concept as:

$$\sigma = f(T°,\ f_1\%, f_2\%) \qquad 3.3$$

This problem is classically tackled by means of a "*trial and error*" approach that requires a large number of produced samples, increasing so the costs and the material deployment time.

Instead, goal of this work is to propose a theoretical approach to face this problem, leading to the individuation of the most influencing parameters and their best combination for optimizing the electrical conductivity.

The concepts of Design of Experiments (DoE), which is responsible for planning the experiments and adopted for our purposes and the Response Surface Methodology (RSM) that allows to obtain an analytical model are presented in the following paragraphs.

3.6 Design of Experiment (DoE) applied to the experimental activity

The techniques of DOE are a systematic approach to obtain the maximum amount of information from various types of experiments trying to minimize the total number of experiments. Many methods are developed and available for different types of applications [5],[7].

In general, the experiments are used to study the performance of processes and systems which can be represented schematically as in Fig.3.11

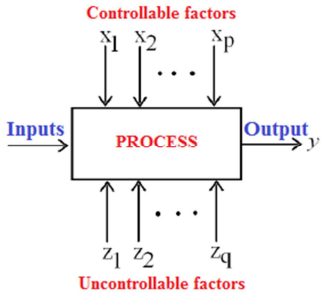

Fig.3.11: General model of a process or system

Briefly, the process can be seen as a combination of machines, methods and other resources that transform inputs into an output that can has one or more observable responses.

Some process variables (x_1, x_2,. ..,x_p) are controllable, whereas other variables (z_1, z_2,…,z_q) are uncontrollable. These variables are called *factors*.

The objectives of the experiment may have the following purposes:

- Evaluating which variables are most influential on the response y.
- Evaluating where to position the controllable variables x so that y is almost always near the desired nominal value or in any case that its variability is minimal.
- Evaluating where to position the controllable variables x so that the variability of y is minimal
- Evaluating where to position the controllable variables x so that it is minimized the influence of uncontrollable variables z on the output y

The first two aims are pursued in the research. In fact, an objective is to identify the parameter that most affects the performance of the composite. Moreover it is also important to identify the combination of parameters that provides the desired response.

The general approach to the planning and realization of an experiment is called "strategy of experimentation".

A strategy widely used is the approach "one-factor-at-time", i.e. changes by a factor at time between an experiment and the next.

However the approach "one-factor-at-time" don't take into account the interaction between the factors and the result is an inefficient approach to the project.

The correct approach is the "factorial" experimentation. A full factorial experiment (as that adopted in our case) is an experiment whose design relies on two or more factors, each with discrete possible values or "levels", and whose experimental units take on all possible combinations of these levels across all such factors. Such an experiment allows studying the effect of each factor on the response variable, as well as the effects of interactions between factors on the response variable. The disadvantage of this variant is that when the number of factors of interest increases, the number of experiments required grows exponentially.

In our case, the parameters of interest and their relative levels are:

- T°, the temperature variable in the range [30-110]°C and with a discretization at 5 levels: [30, 50, 70, 90, 110]°C;

- f_1%, the carbon nanotubes content (CNTs), variable in the range [0.05-1]% with a discretization at 5 levels, [0.05, 0.1, 0.3, 0.5, 1]%;
- f_2%, the clay content (HT), variable in the range [0-1]% with a discretization at 3 levels, [0, 0.1, 1]%.

In this context, Dex Scatter Plot (DSP) and Main factor Plot (MfP) are tipically graphics used for the representation of the processed data.

The Design of experiment (Dex) Scatter Plot is a graphic technique very useful in determining which are the most important factors influencing the response function.

The DSP shows the values of the response function for selected levels of each independent variable for different combinations of levels of the remaining variables. The graphical results are shown in Fig.3.12. For example, just to suggest a reading indication, in the left graph of the same figure, for each value of CNT concentration available (0.05 0.1 0.3 0.5 1 %) is plotted the conductivity obtained varying the other two parameters, temperature and HT concentration, in all their possible combinations.Instead, the Main factor Plot (MfP) is a graphic technique that allows to detects the dependency order, the direction of dependency and eventual independence from each factor (see Fig. 3.13). It is obtained frm the DSP by considering the escursion at the lower and higher level for each parameter and by graphing the segment between the corresponding mean value. The slope of this straight-line represents the influence of the particular design parameter on the performance function. A null value indicates the indipendences; a positive/negative gives information about the direction of the dependence (increasing/decreasing). A higher value corresponds to a higher dependency order.

From the analysis of these graphical representations, it is possible to observe that the final conductivity of the composite, is strongly positive influenced by the concentration of the conductive filler (f1%) as can be expected. In fact, the MfP in Fig.3.13 reports a straight-line with a positive high slope for the design parameter f_1%. It also detects a significant positive dependence of the conductivity from the inert filler (f2%) and a weak positive influence from the temperature (T°). In fact, the MfP for f_2% and T° highlights a positive slope, very small for the temperature.

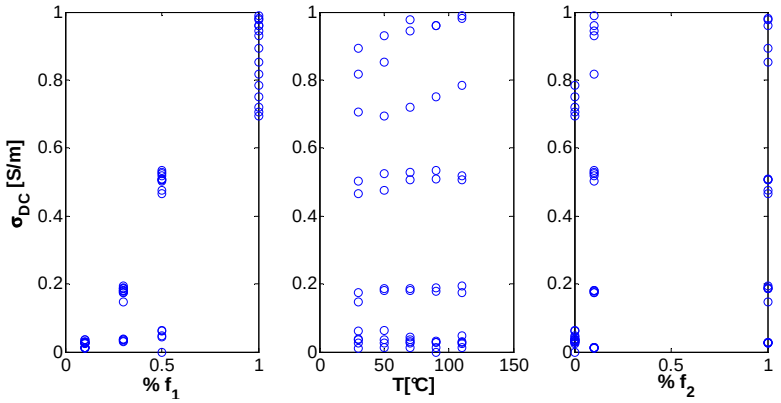

Fig.3.12: DSP for measurements results

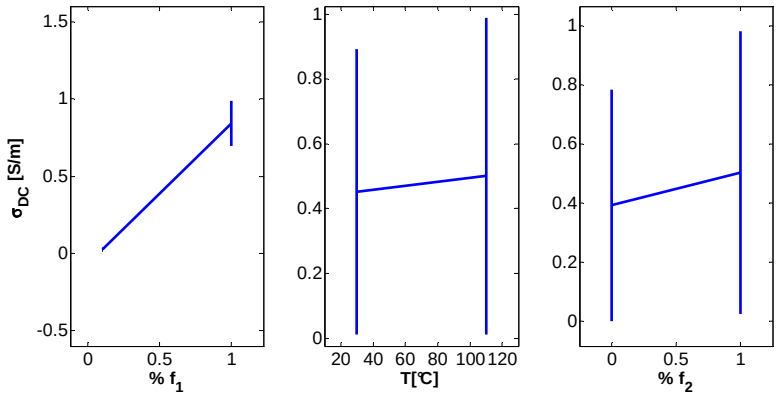

Fig.3.13: MfP for measurements results

3.7 Response Surface Methods (RSM) for performance optimization

Response Surface Method (RSM) is a collection of mathematical and statistical techniques that are useful for developing, improving and optimizing a product or process [8].

RSM finds applications in the industrial world, particularly in situations where several input variables potentially influence some

performance or characteristic of the product/process. This measure of performance or feature is called *response*.

The input variables are called *independent variables* or *factors*, and are subject to the control of the designer, at least during the test phase. The term Response Surface Methodology derives from the use of the graphical representation of the response as a function of the independent variables.

Since the shape of the true response function f is unknown, it is necessary to obtain an approximation and the effectiveness of the RSM strongly depends on the ability of designer to develop adequately this approximation.

Typically, a polynomial model of low order results appropriate. This empirical model is called Response Surface Model.

In many cases polynomial models of the first or second order (as in our case) are requested while in other situations polynomial approximations of order higher than second are used.

A second order model have an expression as:

$$\mu = \beta_0 + \sum_{j=1}^{k} \beta_j x_j + \sum_{j=1}^{k} \beta_{jj} x_j^2 + \sum_{i=1}^{k} \sum_{\substack{j=2 \\ j>i}}^{k} \beta_{ij} x_i x_j \qquad 3.4$$

This technique applied to the collected experimental results allows to derive the graphical representation of the response of interest (DC conductivity) as a function of each independent parameter (T°, f1%, f2%) as shown in Fig.3.14.

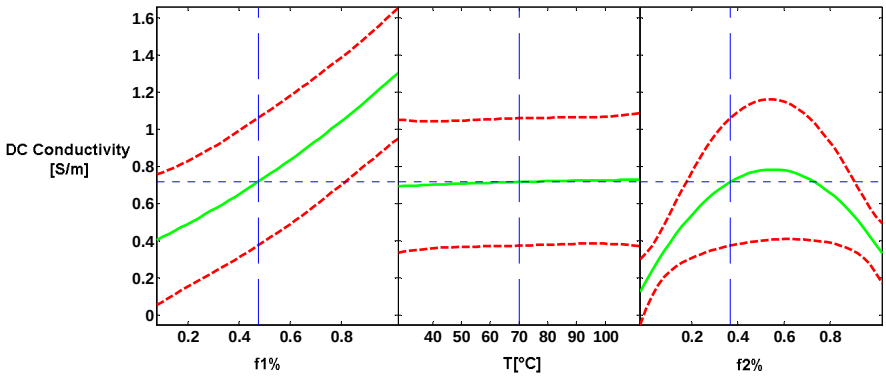

Fig.3.14: RSM obtained by measurement data

The analysis of this graph allows interesting observations. As regards the variation of the conductivity due to the variation of the carbon nanotubes content (f_1%) it is possible to observe a dependency approximately linear.

This is also expectable observing the conductivity law. In fact, when the concentration of conductive filler increases, up to the extreme case of 100%, the conductivity of the composite tends to that of the filler.

$$\sigma_m = \sigma_c(\Phi - \Phi_c)^t \quad \rightarrow \quad \sigma_m \approx \sigma_c \quad when \quad \Phi \rightarrow 1 \qquad 3.5$$

The temperature dependence appears not particularly relevant. Instead, of particular interest is the predicted trend of the conductivity as a function of the nanoclay concentration (f_2%) which appears of a parabolic type.

This means, if the prediction is correct, that there is a concentration of HT (around 0.6 wt%), intermediate to that employed in the production of the observed samples, in correspondence of which the composite conductivity is maximum, as highlighted in Fig.3.15.

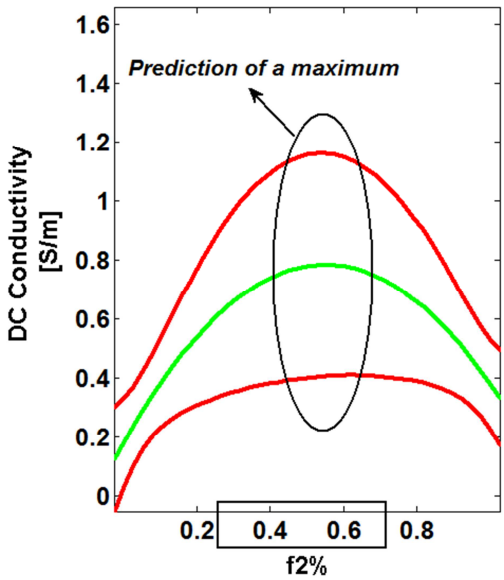

Fig.3. 15: Prediction of a maximum for the conductivity

A 3D representation of the response surface for the conductivity related to the clay concentration is reported in Fig.3.16

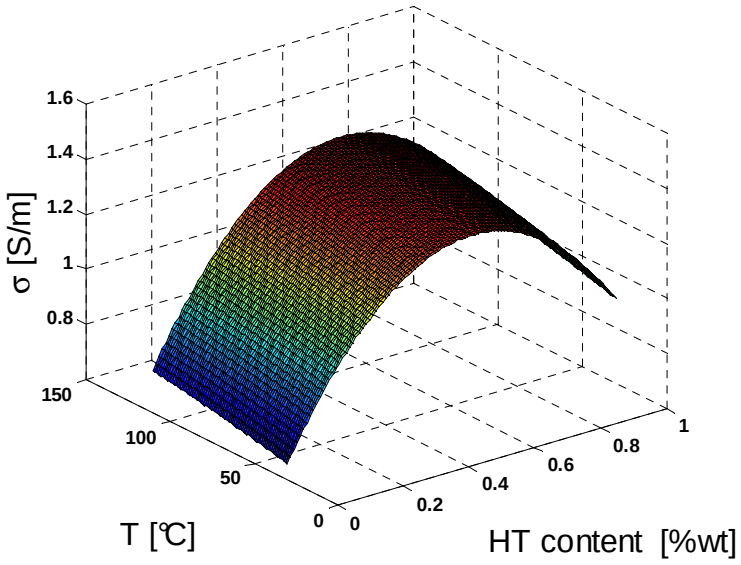

Fig.3.16: 3D response surface

It is possible to conclude that for maximizing the conductivity, a a 1 wt% of CNT and around 0.6 wt% of HT must be adopted.

3.8 Experimental verification

Only the experimental characterization can confirms the theoretical prediction.

Therefore, in order to verify the predicted "optimized" parameters design, a set of additional composites, having a definite composition, was required and kindly provided by UNISA_DICA Unit. Their characteristics are reported in Table 3.7

Table 3 7: Samples on request

Samples	% CNT	Type of CNT	% Clay	Type of Clay	Total charge	Thickness[mm]
Epoxy-80DDS-0.3HT	1	MWCNT	0.3	Hydrotalcite	1.03	2.26
Epoxy-80DDS-0.5HT	1	MWCNT	0.5	Hydrotalcite	1.05	2.29
Epoxy-80DDS-0.7HT	1	MWCNT	0.7	Hydrotalcite	1.07	2.14

As can be seen, from the data in Table 3.7, to maximize the conductivity composite, the concentration of nanotubes was fixed at 1 wt%. For the clay, three values around this concentration that ideally maximize the performance function (σ) have been committed (0.3, 0.5 and 0.7 wt%). For a correct comparison these samples were electrically characterized in the same conditions as the others.

The measurements of the DC conductivity vs all concentrations of Hydrotalcite now available is shown in Fig.3.17.

The results are really interesting because it is experimentally confirmed that there is a suitable concentration for the clay that must be used for the production of a composite so that it can presents the highest conductivity.

The collocation of the experimental results respect to the estimated response surface is shown in Fig.3.18.

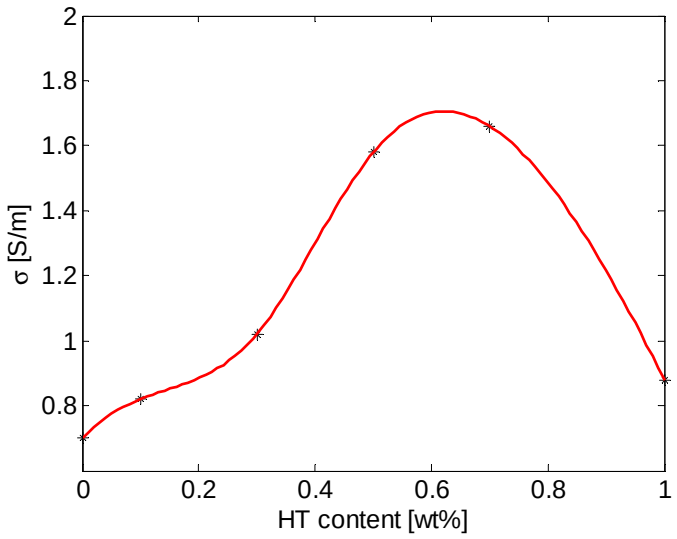

Fig.3.17: DC conductivity vs HT content, experimental data

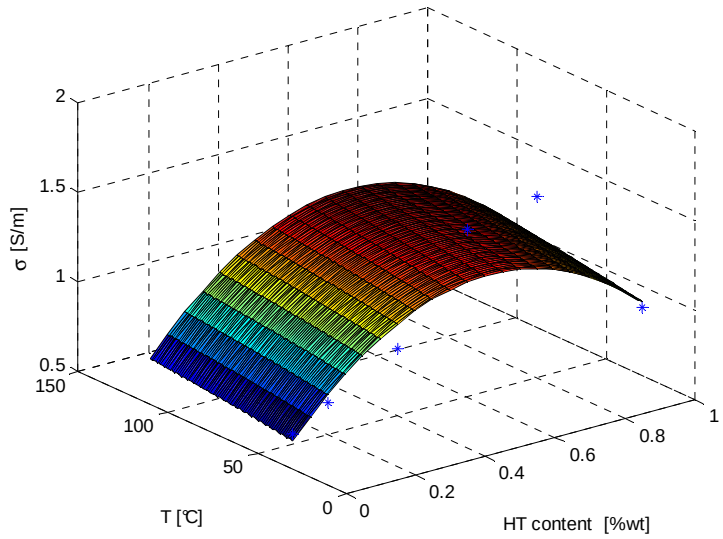

Fig.3.18: Experimental results (*) and response surface

The adoption of this approach, in the experimental field, aims to "ad hoc design" of the material. In fact, until now, the composite is first created and then characterized to determine its performance.

Instead the research efforts aim to predict the performance of the composite through an accurate theoretical study and subsequently to request the production of the composite, with the identified specifications, to have an experimental confirmation.

References

[1] L. Guadagno, B. De Vivo, A. Di Bartolomeo, P. Lamberti, A. Sorrentino, V. Tucci, L. Vertuccio, V. Vittoria, “Effect of functionalization on the thermo-mechanical and electrical behavior of multi-wall carbon nanotube/epoxy composites, Carbon 49, pp. 1919-1930, 2011.

[2] Junjie Wu, D. S. McLachlan, “Percolation exponents and thresholds obtained from the nearly ideal continuum percolation system graphite-boron nitride”, Physical Review B Volume 56, Number 3,pp.1236-1248,1997.

[3] C.W. Nan, Y. Shen, Jing Ma, “Physical Properties of Composites Near Percolation”, Annu. Rev. Mater. Res. 40, pp.131–151, 2010.

[4]P.Lamberti, V.Tucci, “Interval approach to robust design”,COMPEL, The International Journal for Computation and Mathematics in Electrical and Electronic Engineering, pp.280-292, 2007.

[5] D. C. Montgomery. “Design and Analysis of Experiments”, John Wiley & Sons, 5th edition,2001

[6] L.Egiziano, P.Lamberti, G.Spagnuolo, V.Tucci, “Robust Design of Electromagnetic Systems based on Interval Taylor Extension applied to a Multiquadric Performance Function”, IEEE Transactions On Magnetics, Vol. 44. pp.1134-1137 ISSN:0018-9464.

[7] P. Lamberti, “Progetto robusto di circuiti a parametri incerti”, PhD.Thesis, University of Salerno, Italy, 2006

[8] R. H. Myers and D. C. Montgomery, “Response Surface Methodology: Process and Product Optimization Using Designed Experiments”, John Wiley and Sons, 2002.

Chapter 4

Numerical Modeling

A complete understanding of the relations linking the electrical properties with the geometrical and physical characteristics of the composite and the topological structures formed is still to be achieved. Therefore, additional efforts aimed at providing further information about the correlations among electrical characteristics and the variable parameters seems valuable. In this vision, one possible approach to overcome such a gap is trying to compare the results of experimental investigations with predictions obtained by suitable numerical models. For this purpose, a structure simulating a polymeric nanocomposite loaded with carbon nanotubes (CNTs) is developed by considering, in a three-dimensional space, a random distribution of impenetrable conducting cylinders inside an insulating cubic matrix. The variation of the electrical conductivity of the composite for different conductive content is estimated through a 3D resistor network.

The tunneling effect between neighbor filler which is deemed responsible of the global conductivity is taken into account. By using a Monte Carlo method, the electrical conductivity and the percolation thresholds of the obtained structures are analyzed as a function of geometrical and physical influencing parameters. And finally, unlike the models available in the literature, the proposed model allows to conduct studies in AC by means of an appropriate 3D network of capacitors.

4.1 Development of the 3D structure

The CNTs have been modelled as straight cylinders having the desired length L [µm] and diameter W [nm],and therefore an aspect ratio AR=L/W, as shown in Fig.4.1.

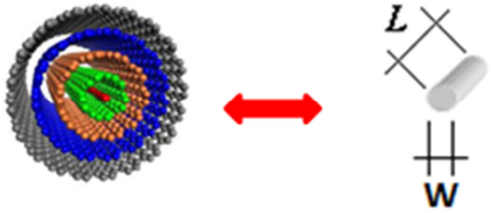

Fig.4.1: Simulation model of the CNT

They are added one at a time, according to an uniform probability distribution, into the 3D elementary cell volume which dimensions are L_x, L_y, L_z, along respectively the x, y and z axes as shown in Fig.4.2.

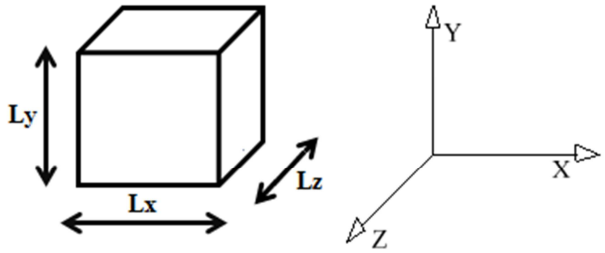

Fig.4.2: 3D elementary cell

More specifically, the cylinders are randomly oriented in space and dispersed in the volume [1]. By indicating respectively with (x_i, y_i, z_i) and (x_f, y_f, z_f), the initial and final axis coordinates of the current dispersed CNT (see Fig. 4.3), the condition of uniformity is ensured by using the following analytical relations:

$$x_i = rand(Y) \cdot L_x\,, \quad y_i = rand(Y) \cdot L_y\,, \quad z_i = rand(Y) \cdot L_z \qquad 4.1$$

$$x_f = x_i + L\emptyset_1 \cos(\mu_1)\,, \quad y_f = y_i + L\emptyset_1 \sin(\mu_1)\,, z_f = z_i + L\vartheta_1 \qquad 4.2$$

where *rand (Y)* is a random number in the interval Y= [0, 1].

Instead, $Ø_1$, μ_1, ϑ_1, are the parameters related to the angular distribution, defined as follows:

$$\vartheta_1 = 1 - 2 \cdot rand(Y),\ Ø_1 = \sqrt{1 - \vartheta_1^2}\ ,\ \mu_1 = 2\pi \cdot rand(Y) \qquad 4.3$$

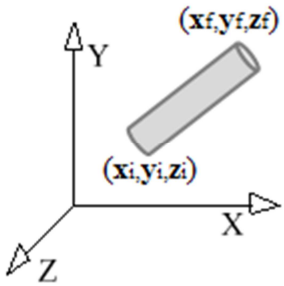

Fig.4.3: Coordinates of the individual CNT

In this generation process, a strict control about the contact, the position or overlap of each CNT (Fig.4.4) is essential for a correct determination of the percolation paths.

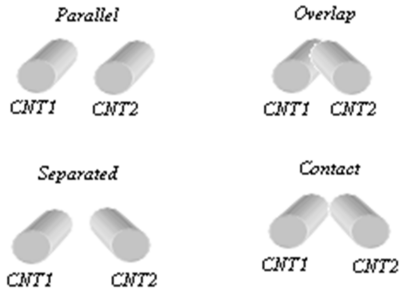

Fig.4.4: Possible positions between the CNTs

Therefore, at each time, before the allocation of a new CNT, a check is made to ensure the physical feasibility, i.e. by controlling that a carbon nanotube cannot penetrate inside the others and that it must be totally contained in the representative volume. A further check is also made on the minimum distance between two CNTs, taking into account the Van der Walls separation (0.34 nm). If this two constraints are not fulfilled by the current CNT, this is automatically deleted and a new one generated again until they are satisfied.

This generation procedure ends when the CNTs have reached a number related to the selected volume fraction established at the start. Typical examples of the obtained structures are shown in Fig.4.5.

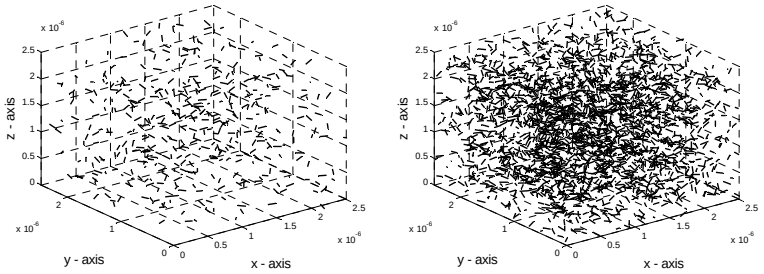

Fig.4.5: 3D simulation cell with straight CNTs at different filler loading (0.015 volume fraction, left ; 0.035 volume fraction right)

4.2 Percolation resistor network

Once the structure is built, the presence of one or more direct path between two opposite sides of the considered cell must be identified.

For this purpose an appropriate search algorithm was adopted. The choice was that of Dijkstra's algorithm[33].

In fact, according to the percolation theory, the presence of at least one available continuous path for the current leads the sharp transition from the insulator behavior to the conductive one.

Due to the unavoidable distances between CNTs and among their clusters the percolation path depends on the definition of a minimum distance consistent with the tunneling phenomenon.

A 3D resistor network model is then introduced to estimate the electrical conductivity.

---

[33] **Dijkstra's algorithm**: conceived by Dutch computer scientist Edsger Dijkstra in 1956 and published in 1959,is a graph search algorithm that solves the single-source shortest path problem for a graph with nonnegative edge path costs, producing a shortest path tree. This algorithm is often used in routing and as a subroutine in other graph algorithms. In particular, the algorithm can be used to partially find the shortest path that joins two nodes of the graph, totally to find those that combine a source node to all other nodes or more times to find all possible paths that connect each node to every other one. This algorithm can be applied in many contexts.

Each branch in the equivalent circuit represents a single percolative path composed of two types of resistors, as shown in Fig. 4.6.

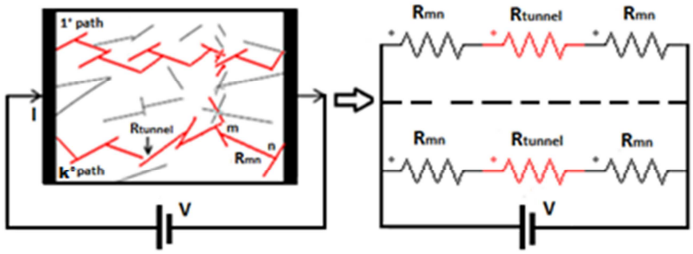

Fig.4.6: 2D view of the conductive paths inside the matrix and the associated resistor network.

R_{mn} takes into account the metallic behaviour of CNT involved in the path and it is simply its intrinsic resistance evaluated with Ohm's law:

$$R_{mn} = \frac{1}{\sigma_{cnt}} \cdot \frac{l_{mn}}{S_{cnt}} \qquad 4.4$$

where σ_{cnt} and S_{cnt} are, respectively, the electrical conductivity and the cross-sectional area of the CNTs, while l_{mn} is the distance between two generic points *m* and *n*.

Typical values of conductivity for multiwall nanotubes (MWCNTs) are in the range $5x10^3$ to 10^6 Sm^{-1}[2].

Due to the unavoidable layer of insulating polymeric materials wrapping around the CNTs, the tunneling effect has been proposed to be the main mechanism responsible of governing the electrical conduction in such polymer nanocomposites.

For this reason a R_{tunnel} is considered in the model for taking into account the charge transport between two consecutive CNTs [3],[4],[5]:

$$R_{tunnel} = \frac{V}{AJ} = \frac{h^2 d}{Ae^2\sqrt{2m\lambda}} exp^{\left(\frac{4\pi d}{h}\sqrt{2m\lambda}\right)} \qquad 4.5$$

where *J* is the the tunnel density current, *A* the CNT cross-section area, *V* the voltage across insulating material, *h* is the Plank's constant , *d* the distance between CNTs, *e* the electron charge, *m* the

mass of electron and λ represents the height of barrier that takes values typically of few eV [6]

From the above expression, it can be noted that tunneling conductance decays exponentially as a function of distance with a characteristic decay length in the order of a few nanometers, typically not larger than 2nm [7].

Finally, once examined the individual conductive branches, the equivalent resistance of all paths in parallel Rtot can be determined and the electrical conductivity (for example along the z axis) can be computed by:

$$\sigma_{comp} = \frac{1}{R_{tot}} \cdot \frac{L_z}{L_x L_y} \qquad 4.6$$

Obviously, to make the obtained data more reliable, a Monte Carlo approach with a sufficient number of simulations is adopted.

The model allows to estimate the average percolation thresholds, the electrical conductivity of composites and the others parameters of interest, for a given CNTs concentration.

4.3 Conductivity numerical results

The electrical conductivity of the composite as a function of the volume fraction of the filler is reported in Fig.4.7.

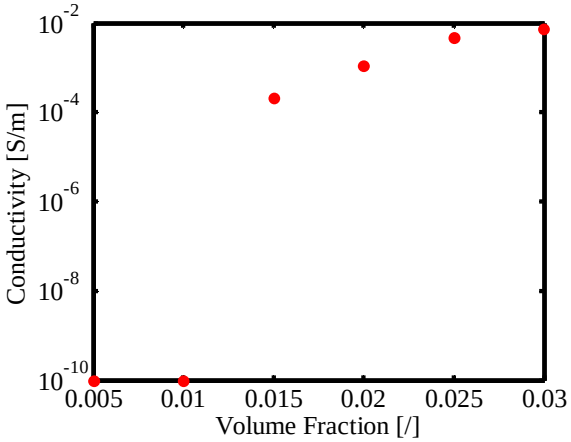

Fig.4..7: Electrical conductivity of the randomly oriented CNT/polymer composites as a function of volume fraction. (CNT AR=100);

According to the classical percolation theory, for low values of the filler content, the composite conductivity is almost that of the pure polymer [8].

As already discussed and now confirmed also by simulations, as soon as the CNTs concentration reaches a critical value, the so-called Electrical Percolation Threshold (EPT), a sharp conductivity jump occurs.

Further increments of the filler content tends to saturate the composite conductivity.

Just to have a feedback of the goodness of our model, the results of our simulations were compared with those obtained from models in the literature [9], as shown in Fig.4.8.

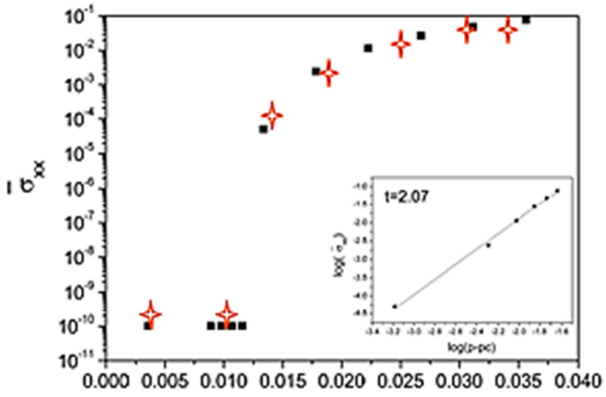

Fig.4.8: DC conductivity: comparison of results with those of literature models. In red our results.

Above percolation, this behavior is described by the general empirical percolation law:

$$\sigma = \sigma_0 (p - p_c)^t \qquad 4.7$$

where σ is the electrical conductivity of the composite, σ_o the theoretical filler conductivity, p the concentration of CNT, p_c the percolation threshold.

The exponent t is a critical parameter depending on the topological complexity of the obtained structure. Values in the range of 1.6-2 are representative of a 3D structure.

From the Fig.4.9 reporting the log-log plot of (4.7), the unknown parameters of the percolation law can be determined

It can be noted that the exponent t (value 1.70) obtained in our simulations reveals a 3D organization of the composite structure.

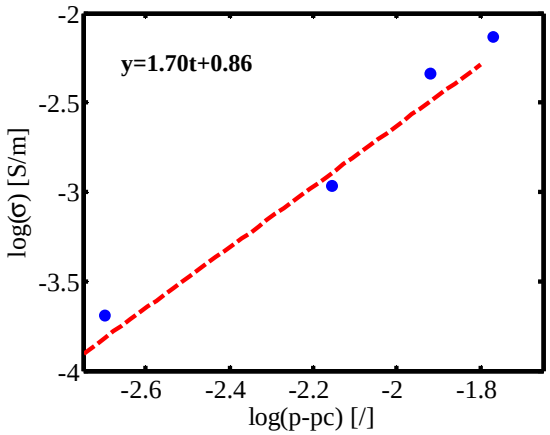

Fig.4.9: log-log plot of the electrical conductivity of the composite as a function of log ($p-p_C$) with a linear interpolation.

4.4 Estimate of electrical percolation threshold (EPT)

From a practical point of view it is important to predict the EPT from the knowledge of the geometrical filler parameters, for example the aspect ratio (AR). In order to evaluate this dependence on the AR, different simulations are made by fixing the reference volume. In Fig. 4.10, it can be observed that the EPT decreases with increasing AR.

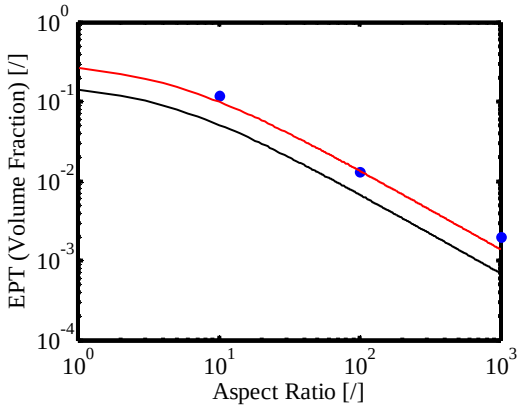

Fig.4.10: Simulated EPT (blue points). The curves are theoretical bounds of the percolation threshold calculated with excluded volume theory.

This is in accordance with theoretical predictions of percolation, namely with the Excluded Volume Theory [10].This theory provides a general relationship between the percolation threshold of systems of various objects and the excluded volume [34]associated with these objects. The results yield predictions for the dependencies, of the percolation critical concentration of various kinds of "sticks," on the stick aspect ratio and the anisotropy of the stick orientation distribution.The usefulness of the this theory for percolation-threshold problems is relevant because this approach gives analytical relationships between the AR and the EPT.

In particular, upper and lower bounds for the percolation threshold are expressed by the following mathematical inequality:

$$1 - e^{\left(-\frac{1.4 \cdot V}{<Ve>}\right)} \leq EPT \leq 1 - e^{\left(-\frac{2.8 \cdot V}{<Ve>}\right)} \qquad 4.8$$

where $< V_e >= \frac{4}{3}\pi W^3 + \frac{2}{\pi}W^2 + \frac{\pi}{2}WL$ is the excluded volume and V is the volume of CNT.

It can be concluded that the Excluded Volume Theory tends to underestimate the EPT with respect to the considered approach, but, according to the evidenced behavior, can be used for a fast EPT estimation by using the following expression:

$$EPT \propto \frac{1}{AR} \qquad 4.9$$

Also in this case is still useful a comparison with other numerical results available in the literature [9], as shown in Fig.4.11

[34] **Exclude volume:** the excluded area (volume) of an object is defined as the area (volume) around an object into which the center of another similar object is not allowed to enter if overlapping of the two objects is to be avoided

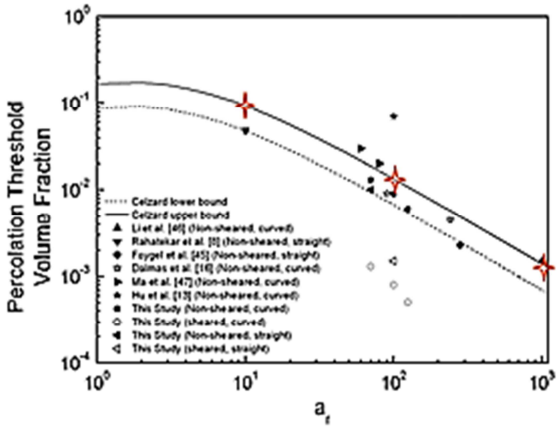

Fig.4.11: EPT:comparison of results with those of literature models. In red our results.

4.5 Variation of parameters and their effects on the conductivity

In addition, in order to predicting the electromagnetic behavior of the composite, the influence of variation of some parameters has been analyzed.

4.5.1 Variation due to CNT conductivity

As already indicated, due to the unavoidable insulating film of matrix material between adjacent nanotubes the tunneling resistance plays an important role in the electrical conductivity of CNTs-based composite whereas the CNT intrinsic conductivity does not exhibit a significant impact.

In fact, as depicted in Fig.4.12, variations in a typical range of the conductivity of the used CNTs, have negligible influence on the final electrical performance of the composite.

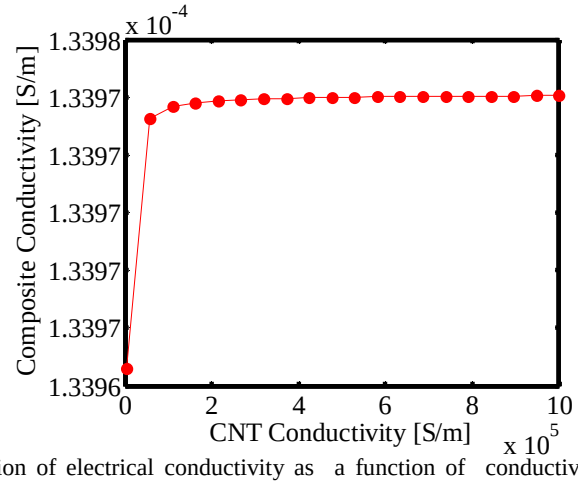

Fig.4.12: Variation of electrical conductivity as a function of conductivity of CNT in a nanocomposite with 0,025 volume fraction of CNTs

4.5.2 Variation due to height of energy barrier

The tunneling effect, as thoroughly discussed in the literature, depends strongly on the separation distance between the CNTs. However, it is also important to consider the height of energy barrier of the host matrix and how its changes affect the conductivity of the composite.

The simulation results are shown in Fig.4.13 considering typical values for a common polymer (epoxy) [10]. These values are strongly influenced by the composite manufacturing processes.

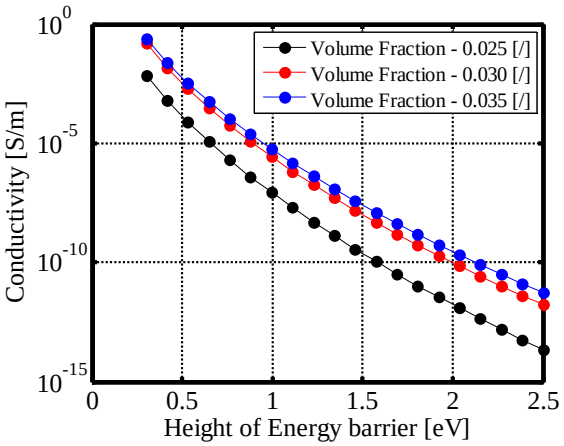

Fig.4.13: Variation of electrical conductivity as a function of the height of barrier for epoxy in a nanocomposite with different volume fraction of CNTs

In this case, it is possible to note how small changes in this parameter cause considerable variations in terms of the final conductivity of the nanocomposite.

A factor of ten in the energy barrier is able to determine a variation of 12 orders of magnitude in the composite conductivity.

One of the major impacts due to this dependence may be an incorrect assumption of the occurrence or non-occurrence of the percolation inside the composite.

In fact, percolation paths could be formed physically, but significant changes in conductivity could not be evidenced. This consideration could also justify the different experimental values, reported in the literature, related to the conductivity and percolation threshold of composites with the same filler and with the same host matrix.

Due to the different manufacturing process of the samples, different values for the energy barrier could have been obtained influencing strongly the tunneling phenomenon impact on the measured electrical conductivity and on the predicted percolation threshold.

4.6 AC numerical model

Due to their light weight, versatility and processability, CNT-based composites are attractive materials for applications as electromagnetic interference (EMI) shielding and then for the production of electronic and electrical devices which satisfy electromagnetic compatibility (EMC) requirements. Therefore the study of composites in the frequency domain and the analysis of their AC properties can provide useful information about this applicability.

In addition to the experimental results the frequency dependent behavior of CNT/epoxy nanocomposite can be modeled by R-C circuit, ,as shown in Fig.4.14.

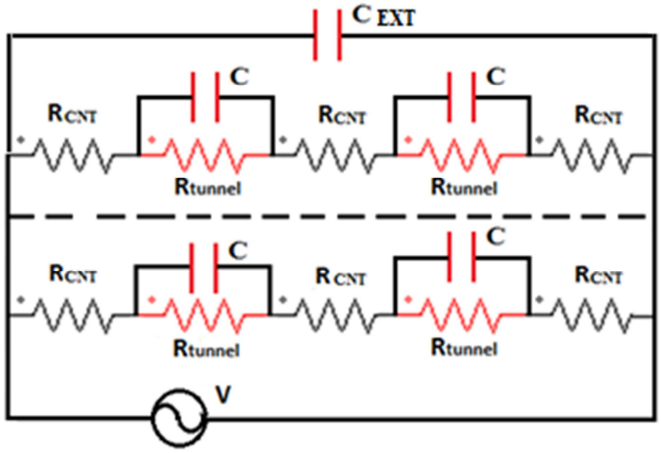

Fig.4.14: R-C model for CNT-based composite

The model is simple and intuitive. Starting point is that in the compound are inevitably established different capacitive effects.

In fact, if we consider for simplicity only two neighbors CNTs, as shown in Fig.4.15, since they are conductors and there is an insulating layer of resin that separates them, the set is structurally a real capacitor.

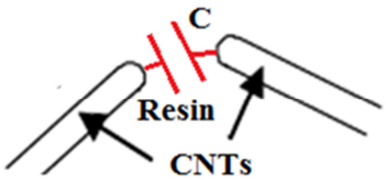

Fig.4.15: Formation of the capacitive effect between CNT

This effect can be taken into account and quantized through the introduction of a capacity C, approximately similar to that of a parallel-plate capacitor, and therefore so evaluated:

$$C = \varepsilon_0 \cdot \varepsilon_r \cdot \frac{A}{d} \qquad 4.10$$

where ε_0 is dielectric constant of the vacuum , ε_r is the dielectric constant of the insulating material, d is the distance between CNTs, and A, with a good approximation, is the cross-sectional area of the carbon nanotube given by:

$$A = \pi \frac{W^2}{4} \qquad 4.11$$

Given the origin of this effect is logical to include these capacitances in parallel to the respective tunneling resistances.

The second capacitive effect is due to the resin confined between the measurement electrodes.

Also in this case, with reference to a parallel-plate capacitor, its contribution is quantized with a capacitance C_{EXT} given by:

$$C_{EXT} = \varepsilon_o \cdot \varepsilon_r \cdot \frac{L_j \cdot L_k}{L_i} \quad with \quad \begin{cases} i = x \; or \; y \; or \; z \\ j \neq k \neq i \end{cases} \qquad 4.12$$

where L_i, L_j, L_k are the dimensions of elementary cell volume along the x, y and z axes, written in this generalized form because there are three different directions (x, y ,z) of interest for the analysis of electrical properties.

4.7 AC observable properties

By using the RC model is possible to have a wide range of information about the behavior of the system in the frequency domain.

All the following illustrations refer to a composite with CNTs at 0.025 volume fraction.

One of the first possibility is the Bode diagram plotting which allows to have the frequency response of the system in terms of its magnitude and phase.

A particular advantage of a simulation model, in the study of this diagrams, is the chance to analyze separately the contribution of the two different capacitive effects, as shown in Fig.4.16

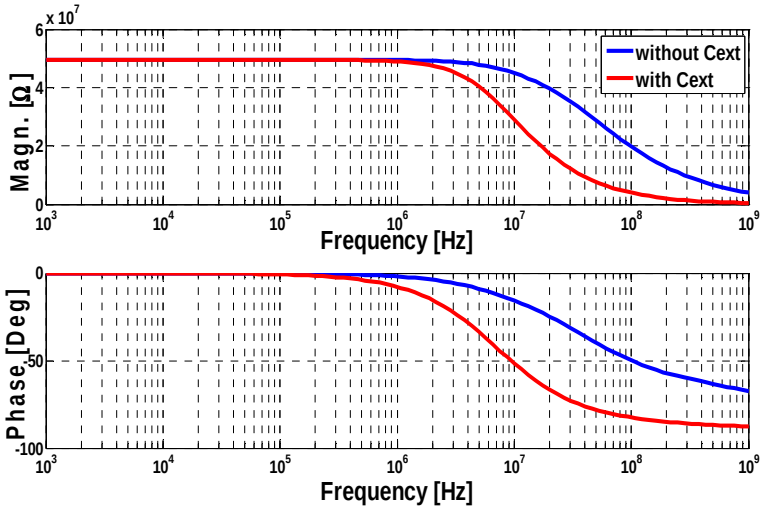

Fig.4.16: Bode plot for the composite with and without the contribution of the external capacitance (CNT content at 0.025 as volume fraction)

Moreover from Bode diagrams, it is possible for example as shown in Fig. 4.17, to investigate also the influences on the final composite behavior due to the potential barrier variations, as previously observed in DC regimen.

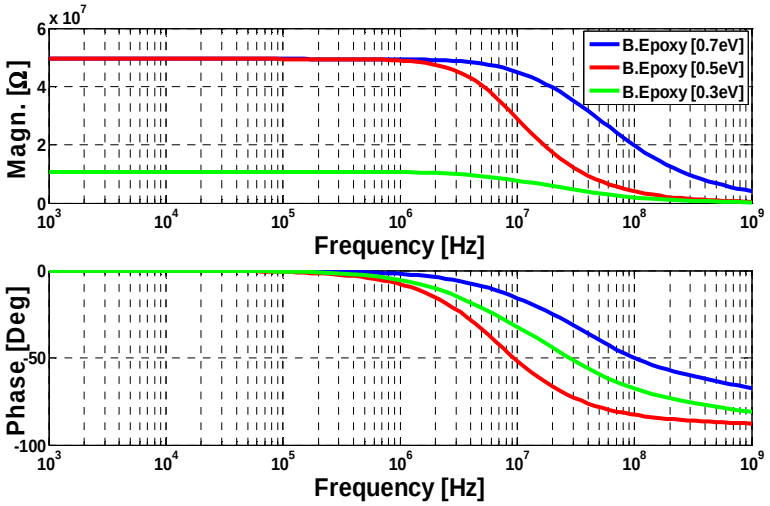

Fig.4. 17: Bode diagram and variations due to potential barrier

Of course in the frequency domain, other classical parameters that provide information useful for the characterization of the composite are, not only the conductivity, but also ε' and ε'', which are respectively the real and imaginary parts of the permittivity.

All these quantities are easily obtainable and analyzable by using the numerical model, as shown in Fig.4.18.

Even for these quantities it is possible to evaluate effects due to variation of the potential barrier since it is considered a crucial parameter for system performance

The Fig. 4.19 shows, for example, these variations for the parameter ε'.

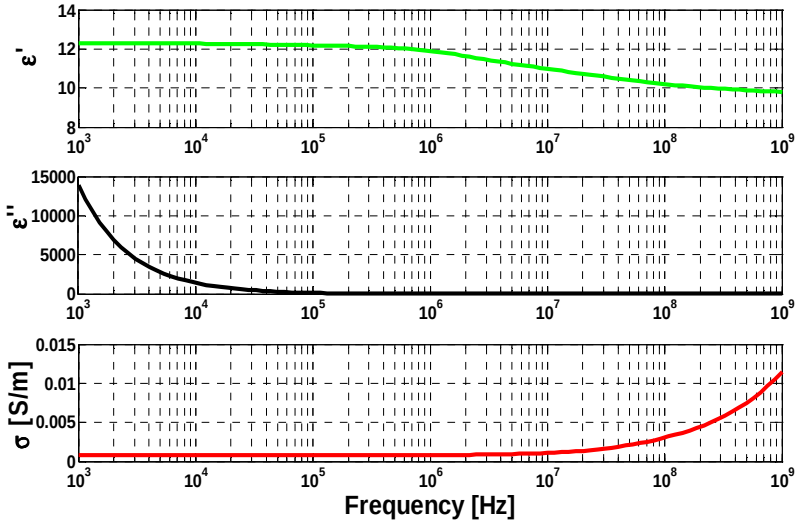

Fig.4. 18: Useful parameters in the frequency domain

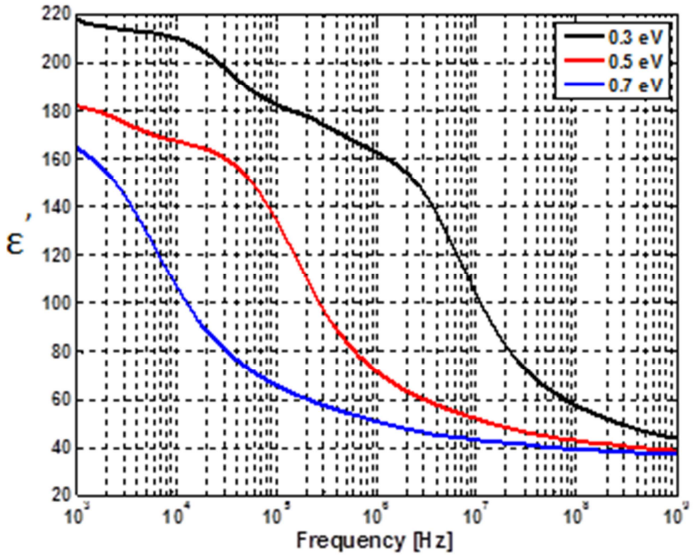

Fig.4. 19: Change in ε' due to potential barrier

4.8 Benefits of the numerical model

Based on a 3D numerical model, the electrical properties of CNT nanocomposites, are predicted in this work. The numerical simulations are based on a resistor network model that takes into account the percolation paths and the tunneling effect.

The electrical conductivity of the nanocomposites with a specific concentration and geometry of the CNTs can be effectively evaluated as well as the percolation law. The excluded volume theory is verified by numerical simulations too.

The numerical analysis has been conducted to investigate the effects of processing parameters and material properties on the electromagnetic behavior of the CNT based-composite, deriving useful hints for the CNT-based composites optimization.

The use of a 3D network of capacitors allows to investigate the behavior of the composite in the frequency domain.

References

[1] A. Allaoui et al., “Mechanical and electrical properties of a MWNT/epoxy composite”, Compos Sci. Techn. 62 (15), pp.1993–98, 2002.

[2] N. Hu et al., “Electrical properties of polymer nanocomposites with carbon nanotube fillers”, Nanotechnology 19,2008.

[3]F. Du et al., “Effect of nanotube alignment on percolation conductivity in carbon nanotube/polymer composites”, Phys. Rev. B (2005) 72:121404.]

[4] C. W. Nan et al., “Physical Properties of Composites Near Percolation”, Annual Review of Materials Research 40 (2010) 131–151.

[5] J. H. Simmons, “Generalized Formula for the Electric Tunnel Effect between Similar Electrodes Separated by a Thin Insulating Film”, Journal of Applied Physics 34 (1963) 1793-1803.

[6] N.Hu et al., “Investigation on sensitivity of a polymer/carbon nanotube composite strain sensor”, Carbon 48, pp.680-687,2010.

[7] C.Li, E. T. Thostenson, Tsu-Wei Chou, “Dominant role of tunneling resistance in the electrical conductivity of carbon nanotube–based composites”, Applied Physics Letters 91, 2007

[8] L. Guadagno et al., “Cure behavior and physical properties of epoxy resin-filled with multiwalled carbon nanotubes”, Journal of Nanoscience and Nanotechnology 10, pp.2686-2693,2010.

[9] A.E.Eken, E.J. Tozzi, D.J. Klingenberg, E. Bauhofer ”A simulation study on the combined effects of nanotube shape and shear flow on the electrical percolation thresholds of carbon nanotube/polymer composites” Journal of Applied Physic 109, April,2011.

[10] I. Balberg et al., “Excluded volume and its relation to the onset of percolation”, Physical Review B 30 (7), pp.3933-3943,1984.

Conclusions

This thesis has been focused on the electromagnetic characterization and modeling of CNT-based composite, a topic of recent interest and highly attractive for its various applications. In fact, in these last years, there has been a strong emphasis on the development of polymeric nanocomposites, a new class of materials characterized by a dispersion of ultrafine phases, typically of the order of a few nanometers. Due to their dispersion, they possess unique properties not shared by conventional composites, offering new technological and economic opportunities ranging from advanced aerospace systems to commodity plastics. Therefore, nanocomposites represent a excellent alternative to the conventional filled polymers and polymer blends. The incorporation of low nanoparticles content, such as carbon nanotubes, have resulted in property enhancements with respect to the neat polymer. This lower loadings favourite processing and reduce composites weight.

Since CNTs can be exploited with varying structural and physical properties, geometry and functionality, an overview on the state of art that collects all these information has been reported.

Moreover, some fundamental phenomena underlying the performances of nanocomposites such as the percolation theory, responsible for the change in their conductivity and the tunneling effect, primary mechanism of electrical conduction in these new materials, have been accurately presented.

Although research activities in CNT-based composites have made enormous progress towards the production of next-generation advanced structural materials, some questions responsible of their properties still remain to be clarified.

For this purpose in this thesis CNT-epoxy systems or multi-phase composites (epoxy/CNT/clay) novelty in literature, have been considered in a wide experimental characterization activity.

The aim of this characterization was to identify possible correlations between morphological characteristics of the different fillers and electrical properties of the nanocomposites. The analysis of the conductivity vs the concentrations of nanofillers (MWCNTs and MWCNTs/HT) have revealed interesting aspects about the percolation threshold and the maximum value obtainable for the conductivity.

The application of the Design of Experiment (DOE), was adopted in order to analyze the combination of factors that maximizes the electrical performance of the composite and in particular its conductivity.

This problem is classically tackled by means of a “trial and error” approach that requires a large number of produced samples, increasing so the costs and the material deployment time.

In fact, until now, the composite is first created and then characterized to determine its performance.

Instead, goal of this work has been to propose a theoretical approach to face this problem, leading to the individuation of the most influencing parameters (between CNT and HT concentrations or temperature) and their best combination for optimizing the electrical conductivity.

Therefore, in order to verify the predicted “optimized” parameters design, a set of further composites having the specifications (concentrations of fillers), identified through this study have been required and then characterized.

The results are really interesting because it is experimentally confirmed that there is a suitable concentration for the clay, as predicted, that must be used for the production of a composite so that it can presents the highest conductivity.

This can give the possibility of having a tailored material as well as build systems with controlled and reproducible properties.

As concern the numerical modeling, it has been developed in order to provide further information about the relations linking the electrical properties with the geometrical and physical characteristics of the composite and the formed topological structures.

This is possible for example by comparing the results of experimental investigations with predictions obtained by suitable numerical models.

For this purpose, in Matlab® enviroment, a 3D structure simulating a polymeric nanocomposite loaded with carbon nanotubes, schematized as cylinders, has been developed.

The variation of the electrical conductivity of the composite for different conductive content was estimated through an associate 3D resistor network. The model take into account also the tunneling effect between neighbor filler.

By using a Monte Carlo method, the electrical conductivity and the percolation thresholds of the obtained structures was analyzed as a function of geometrical and physical influencing parameters.

These simulations have shown, for example, a strong influence on the composite performances by the variations of the energy barrier, a topic that is still not fully explored in the literature and thus it deserves attention.

Unlike the models available in the literature, the proposed model allows to conduct studies in AC by means of an appropriate 3D network of capacitors.

Also in this case, in addition to the obvious comparison with the experimental data, it is possible, for example, simulate and evaluate the impact of the dispersion of CNT on the permittivity of the composite even for different values of geometric and production parameters. Moreover, it is possible to obtain, in easy way, the Bode plot for information about the frequency response of the system in terms of its magnitude and phase or to investigate the conductivity in the frequency domain.

Acknowledgments

First of all, I ought to thank Prof. L.Egiziano and Prof. V.Tucci that in addition to give me the opportunity, the attention and the confidence to work with them, helped me to grow even more in my scientific education. For their style, they are an example not only professional for young researchers. Thank you very much!

I wish to thank my official tutor, Eng. P. Lamberti, who provided me with guidance, suggestions and assistance always with a caring approach. She has been the guiding light in my carrier as a PhD student.

I want to thank also Eng. A. Giustiniani for sharing with me his research philosophy and approaches, turning ideas into practical solutions and useful tips for my dissertation.

My thanks go also to the lab staff, Eng. R. Raimo and Eng. B. De Vivo, for their support and advice that greatly facilitated and gladdened this my experience. They have been like true friends before than colleagues.

I want also to thank all the other Professors of the DIEII for their fruitful teachings and ad hoc lessons.

Last but not the least, I wish to thank my family and my girlfriend for their estimation and their encouragements throughout my PhD program.
I owe my parents, Clara and Mario, much of what I have become. They taught me the honesty and respect values above all other virtues.
I thank Federica for her love, her support, and her confidence throughout the last six years.
I dedicate this work to them, to honor their love, patience, and support during these years.

I have worked hard to achieve my goals in life, I thank God and my beloved Saint Pio of Pietrelcina for giving me this force!

The list can be endless… I thank all who gave me also a simple smile.